

Calcium Transients in Dendritic Spines
Ekta Dadlani, Shayan Raofi, and Tyler Bodily

Supplementary Material

Supplementary Equations S1

Ryanodine Receptors from Leung et al.

Equations	Significance
$T = \omega_\infty / K_d$, $T(d\omega/dt) = \omega_\infty - \omega$	The Relaxation Time of RyR
$\omega = 1 - P_{C2}$	Fraction of Ryanodine channels that are not in the closed (C2) state
$\omega_\infty = (1 + K_a^4 / Ca_{cyto}^4 + Ca_{cyto}^3 / K_b^3) / (1 + (1 / K_c) + K_a^4 / Ca_{cyto}^4 + Ca_{cyto}^3 / K_b^3)$	Equilibrium between ω and T
$P_o = \omega(1 + Ca_{cyto}^3 / K_b^3) / K_a^4 / Ca_{cyto}^4 + 1 + Ca_{cyto}^3 / K_b^3$	Open probability of RyR (dependent on the Ca_{cyto} concentration because this is a CICR dependent process)
$J_{RYR} = (V_{RYR} P_o + V_{leak})(Ca_{ER}^{2+} - Ca_{cyto}^{2+})$	Flux of Ca^{2+} from the ER to the Cytoplasm via RyR

Neck Flux from Cugno et al.

Equations	Significance
$J_{Neck} = KN(Ca_{cyto}^{2+})$	Efflux of Ca^{2+} from the neck of the spine

Supplementary Equations. S2

Cytosolic Flux

$$\frac{\partial [B_m]}{\partial t} = D_{B_m} \nabla^2 [B_m] - k_{B_{m,on}} [Ca^{2+}] [B_m] + k_{B_{m,off}} [CaB_m],$$

and

$$\frac{\partial [CaB_m]}{\partial t} = D_{CaB_m} \nabla^2 [CaB_m] + k_{B_{m,on}} [Ca^{2+}] [B_m] - k_{B_{m,off}} [CaB_m]$$

And include diffusive constants from previous literature.

The NMDAR equations are as follows:

$$\zeta_i = \frac{G_0 + n_0 h}{1 + \frac{n_0 h}{g_\infty}}.$$

Where ζ is the single channel conductance, G_o is the minimum conductance, g_{inf} is the maximum conductance, n_o corresponds to extracellular calcium activity and equals $0.5 * [Ca^{2+}]$

$$G_{NMDAR} = \frac{\zeta_i \times 10^{19}}{(2 \times 1.602) \times 6.022 \times 10^{23}} \left[\frac{Ca^{2+} moles}{V \cdot s} \right]$$

Single channel conductance is changed to conductance per mole of NMDARs

$$J_{NMDAR} = \gamma_i \frac{N_{NMDAR}}{\beta_{NMDAR} A_{PSD}}$$

The flux is dependent on the amount of NMDARs, the area of the PSD, and channel dynamics γ_i .

$$\gamma_i = P_0 G_{NMDAR} \left(I_f H(t) e^{-t/\tau_f} + I_s H(t) e^{-t/\tau_s} \right) B(V_m) (V_m - V_r),$$

$$B(V) = \frac{1}{1 + e^{-K_m V_m} \left(\frac{[Mg]}{Mg_{scale}} \right)}$$

From previous studies.

The VSCC equations are:

$$J_{VSCC} = k_{Ca^{2+}}(V_m(t)) \cdot [VSCC] \cdot (e^{-\alpha_4 t} - e^{-\beta_4 t})$$

Which is the flux of calcium through the channels, and as such is dependent on channel density and is modulated by a bioexponential based on previous studies. k_{Ca} , the single channel dynamics, is given by:

$$k_{Ca^{2+}}(V_m) = \frac{\gamma V_m(t) N_A \left(0.393 - e^{\frac{-V_m(t)}{80.36}} \right)}{2F \left(1 - e^{\frac{-V_m(t)}{80.36}} \right)}$$

And is voltage dependent.

Both channels are influenced by the change in membrane voltage via EPSP and BPAP:

$$V_m(t) = V_{rest} + BPAP(t) + EPSP(t)$$

Where

$$BPAP(t) = maxBPAP \left(I_{bsf} e^{-(t-tdelaybp)/t_{bsf}} + I_{bss} e^{-(t-tdelaybp)/t_{bss}} \right)$$

And

$$EPSP(t) = s_{term} \left(e^{-(t-tdelay)/t_{ep1}} - e^{-(t-tdelay)/t_{ep2}} \right)$$

There is also Calcium flux out of the plasma membrane, which is given by sodium calcium exchanger (NCX) and calcium ATP pump, PMCA. NCX harnesses the sodium electrochemical gradient, bringing in 3 sodiuns in order to move one calcium against its electrochemical gradient. Extracellular sodium is also considered to be an infinite source, and as such it is not considered in the NCX flux equation.

$$J_{NCX} = \beta_i \beta_{NCX} \left(\frac{V_{maxr22} [Ca_{cyto}]}{K_{mr22} + [Ca_{cyto}]} \right) n_{PM_r}$$

PMCA simply removes calcium from the cytosol and into the extracellular space at the cost of ATP.

$$J_{PMCA} = \beta_i \beta_{PMCA} \left(\frac{V_{maxlr23} [Ca_{cyto}]^2}{K_{mlr23}^2 + [Ca_{cyto}]^2} + \frac{V_{maxhr23} [Ca_{cyto}]^5}{K_{mhr23}^5 + [Ca_{cyto}]^5} \right) n_{PM_r}$$

For both of these equations, they are multiplied by:

$$\beta_i = \left(1 + \frac{P_{rtote} \cdot K_{me}}{(K_{me} + [Ca_{cyto}])^2} + \frac{P_{rtote} \cdot K_{mx}}{(K_{mx} + [Ca_{cyto}])^2} \right)^{-1}$$

K and P are all constants, and n_{PM_r} changes the units to a membrane flux:

$$\frac{vol_{cyto_r}}{area_{PM_r}}$$

NCX and PMCA are distributed uniformly across the plasma membrane like VSCCs.

Fixed buffers are modeled in a similar way to the mobile buffers, only diffusion is not taken into account and their rate kinetics differ to match previous studies:

$$J_{B_f} = k_{B_{f,on}} [Ca^{2+}] [B_f] - k_{B_{f,off}} [CaB_f]$$

$$\frac{\partial [B_f]}{\partial t} = -k_{B_{f,on}} [Ca^{2+}] [B_f] + k_{B_{f,off}} [CaB_f]$$

$$\frac{\partial [CaB_f]}{\partial t} = k_{B_{f,on}} [Ca^{2+}] [B_f] - k_{B_{f,off}} [CaB_f]$$

In which $[Ca^{2+}] + [B_f] \rightleftharpoons [CaB_f]$ with the forward rate constant being $k_{B_{f,on}}$ and the reverse rate constant being $k_{B_{f,off}}$.

Taken together, the plasma membrane boundary condition is now:

$$-D(n \cdot \nabla [Ca^{2+}])|_{PM} = f_{in}(NMDAR, VSCC) - f_{out}(PMCA, NCX) - f_{on}(B_f)$$

From Bell et al.

Constants and parameters S3:

Variable	Value	Units
	0.1	μM
$[\text{Ca}^{2+}]_{ER}^{IC}$	60	μM
$[\text{Ca}^{2+}]_{ECS}^{IC}$	2	mM
τ_{cyto}	20	ms
$D_{\text{Ca}^{2+}}$	220	$\frac{\mu\text{m}^2}{\text{s}}$
$k_{Bf, on}$	1	$\frac{1}{\mu\text{M}\cdot\text{s}}$
$k_{Bf, off}$	2	$\frac{1}{\text{s}}$
$k_{B_m, on}$	1	$\frac{1}{\mu\text{M}\cdot\text{s}}$
$k_{B_m, off}$	1	$\frac{1}{\text{s}}$
D_{B_m}	20	$\frac{\mu\text{m}^2}{\text{s}}$
$D_{\text{Ca}B_m}$	20	$\frac{\mu\text{m}^2}{\text{s}}$
$B_{m_{IC}}$	20	μM
$B_{f_{IC}}$	$78.7 \cdot n_{PMr}$	$(\mu\text{M}) \cdot (\text{m})$

Constants for the volumes from Bell et al.

Parameters for RyRs from Leung et al

Parameter	Value	Units	Significance
V_{leak}	0.15	1/s	Rate of the leak of Ca^{2+} from the ER
K_a^4	0.019	μM^4	Dissociation constant
K_b^3	0.257	μM^3	Dissociation constant
K_c	0.057	Unitless	Dissociation constant
K_d	0.1	1/s	Rate for the transition between open RyR and closed RyR
V_{RYR}	5	1/s	Rate of Ca^{2+} flux from the ER to the cytosol via the RyR

Parameter for Neck Flux from Cugno et al.

Parameter	Value	Units	Significance
K_N	1	$\mu\text{m/s}$	Outlet flux velocity

Variable	Value
V_r	-65 mV
maxBPAP	38 mV
tdelaybp	2 ms
$'bsf$	0.75
$'bss$	0.25
$tbsf$	3 ms
tbs	25 ms
s_{term}	25 mV
tdelay	0 ms
tep1	50 ms
tep2	5 ms

Membrane voltage parameters from Bell et al

Variable	Value
N_A	6.022×10^{23} ions/mole
γ	3.72 pS
F	96485.332 C/mole
α_4	34.7 ms^{-1}
β_4	3.68 ms^{-1}
[VSCC]	$2/(6.022 \times 10^{23})$ moles/ μm^2

Parameters for VSCCs from Bell et al.

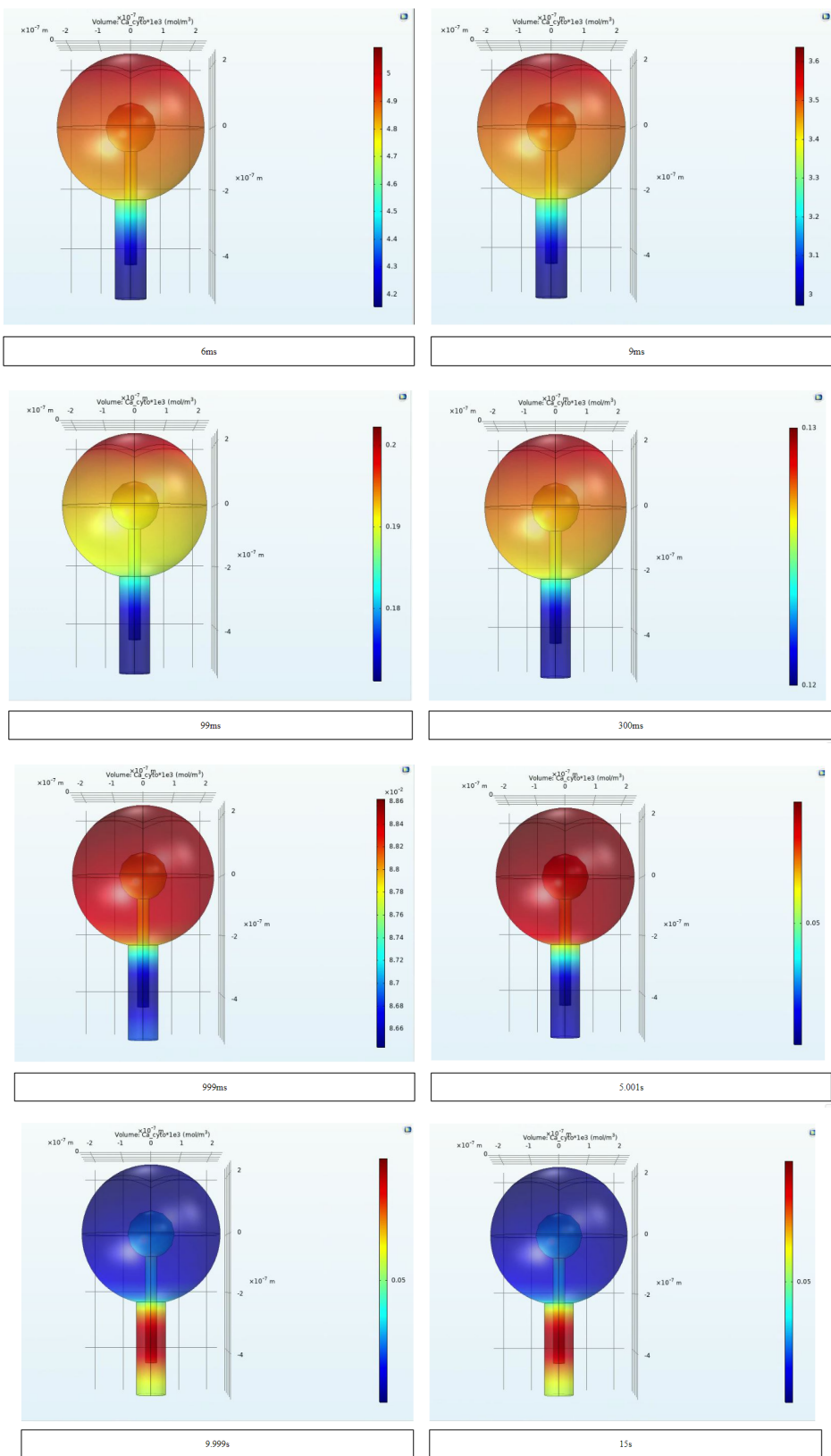
Variable	Value
P_{rtote}	$1.91 \times 10^2 \mu\text{M}$
K_{me}	$2.43 \mu\text{M}$
P_{rtotx}	$8.77 \mu\text{M}$
K_{mx}	$0.139 \mu\text{M}$
$V_{maxlr23}$	$0.113 \mu\text{M/s}$
K_{mlr23}	$0.442 \mu\text{M}$
$V_{maxhr23}$	$0.59 \mu\text{M/s}$
K_{mhr23}	$0.442 \mu\text{M}$
V_{maxr22}	$0.1 \mu\text{M/s}$
K_{mr22}	$1 \mu\text{M}$
β_{PMCA}	100
β_{NCX}	1,000
n_{PMr}	$0.1011 \mu\text{m}$
vol_{cyto}^r	$0.67 \mu\text{m}^3$
$area_{PMr}$	$6.63 \mu\text{m}^2$

PMCA and NCX parameters from Bell et al.

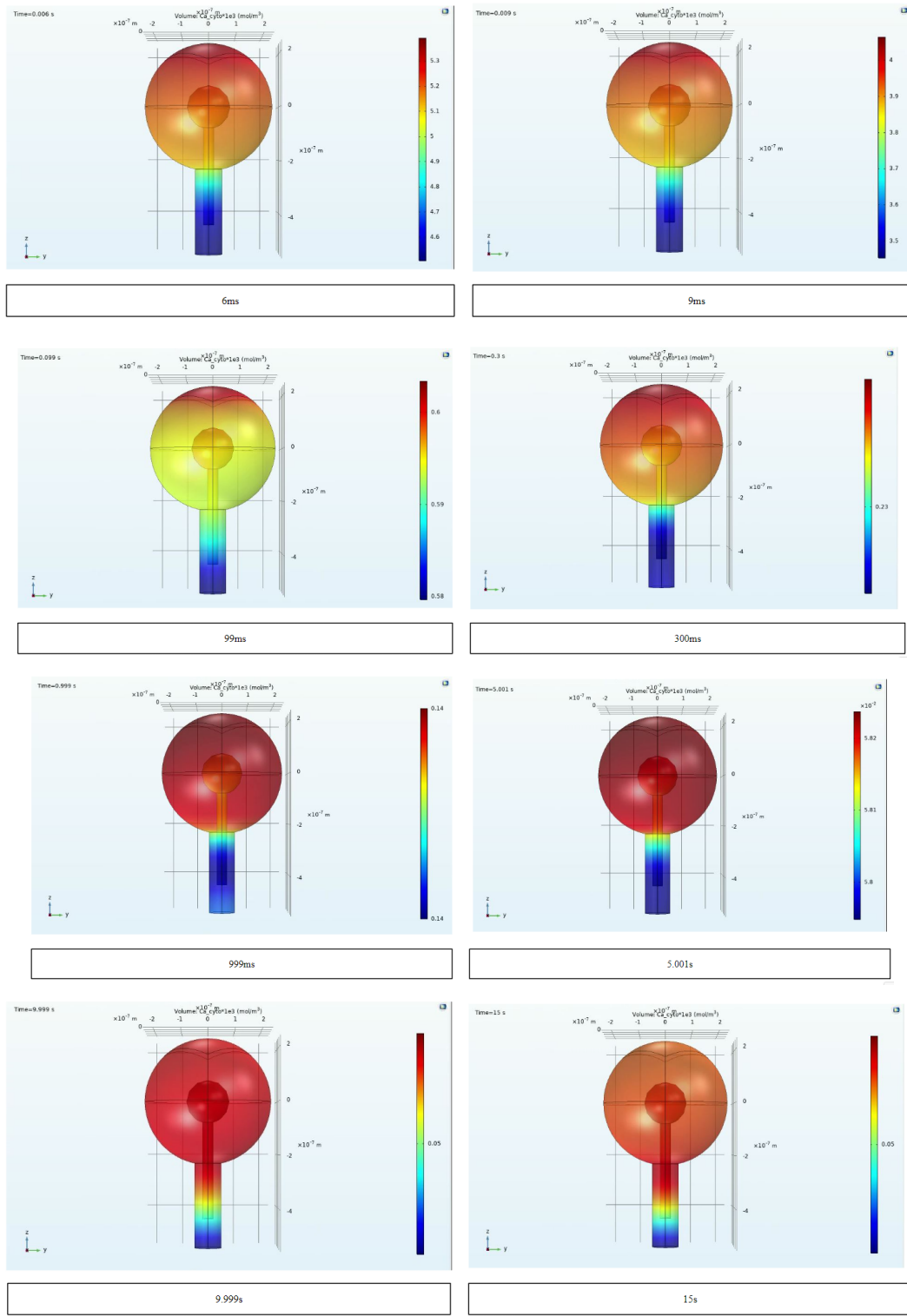
Variable	Value
v_{maxr19}	$1.14 \cdot 10^2 \mu\text{M}/\text{s}$
K_{Pr19}	$0.2 \mu\text{M}$
β_{SERCA}	1,000
n_{SpAppr}	$0.0113 \mu\text{m}$
V_{ol}^{SpAppr}	$0.027132 \mu\text{m}^3$
A_{area}^{SpAppr}	$2.4004 \mu\text{m}^2$
k_{leak}	$0.1608 1/\text{s}$

SERCA parameters from Bell et al.

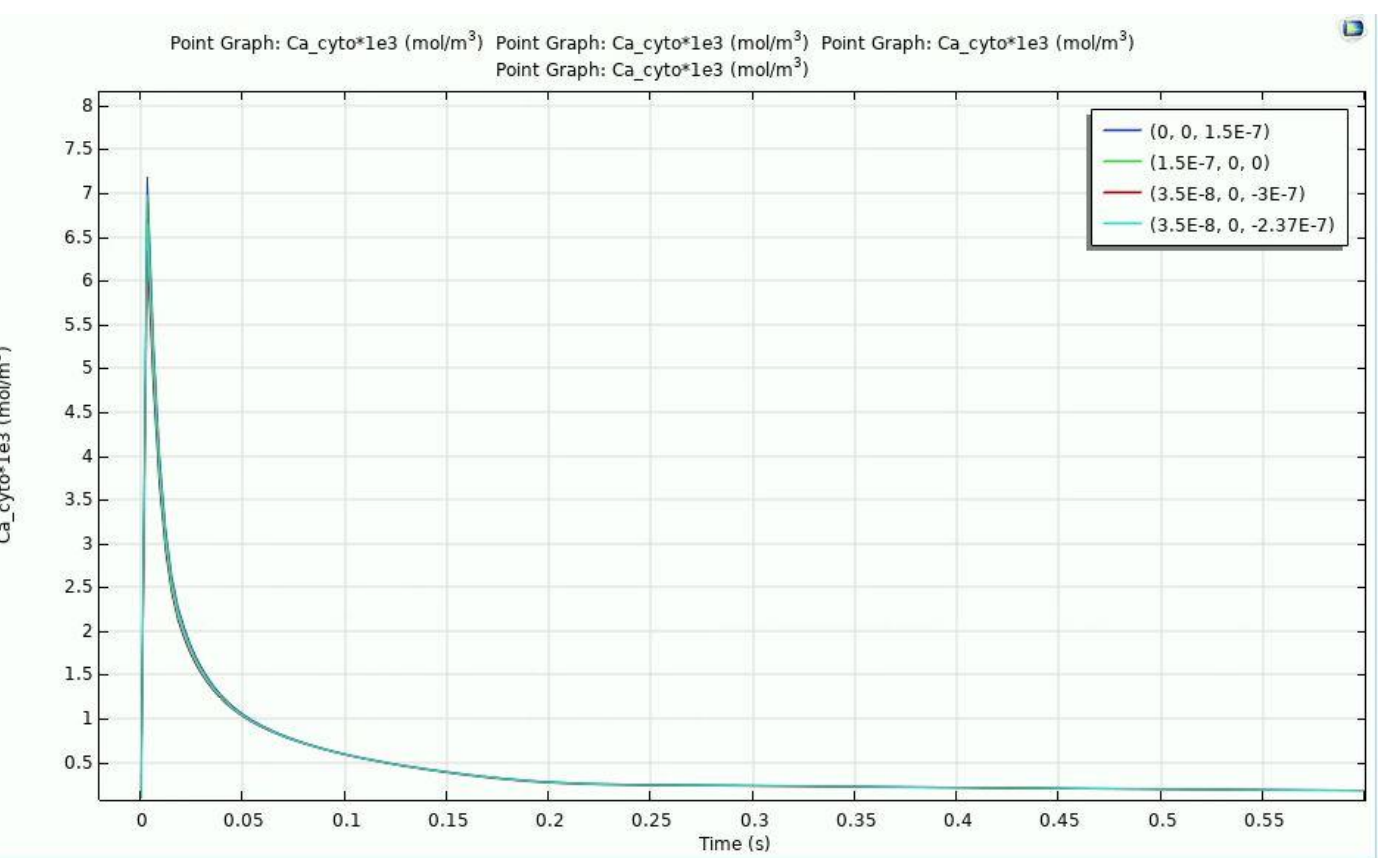
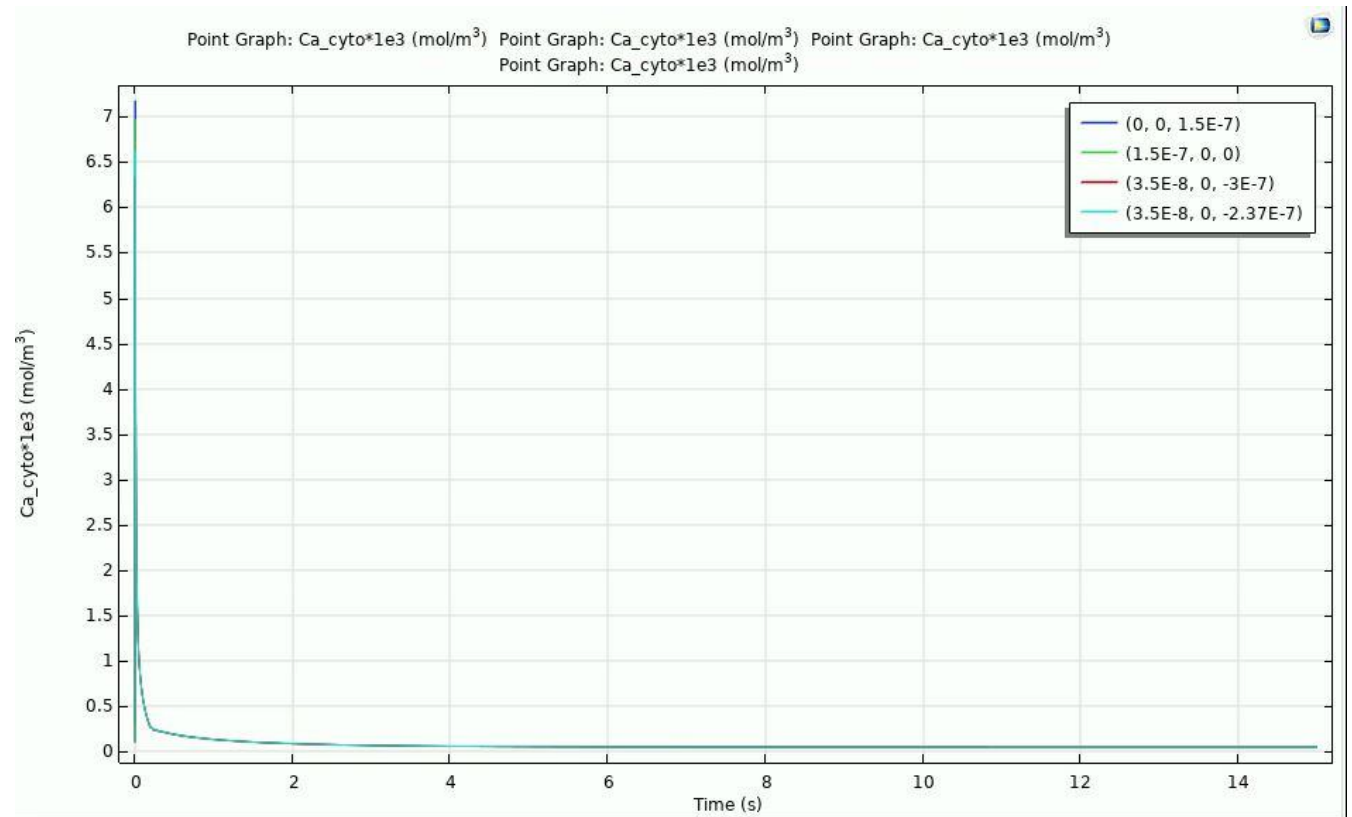
Results in Full: Sphere in Sphere: S4

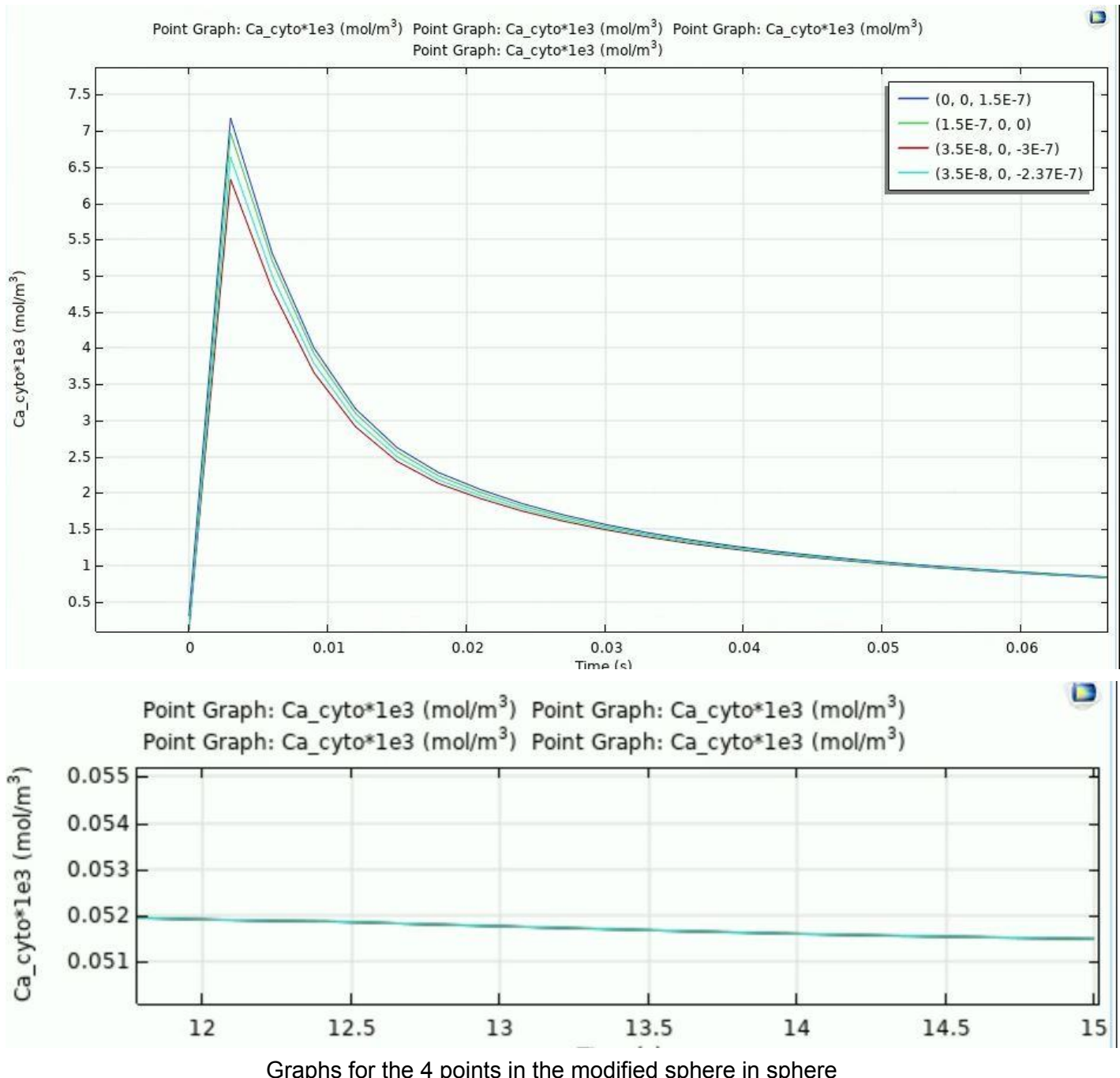


3D plots for the Original Sphere in Sphere Model

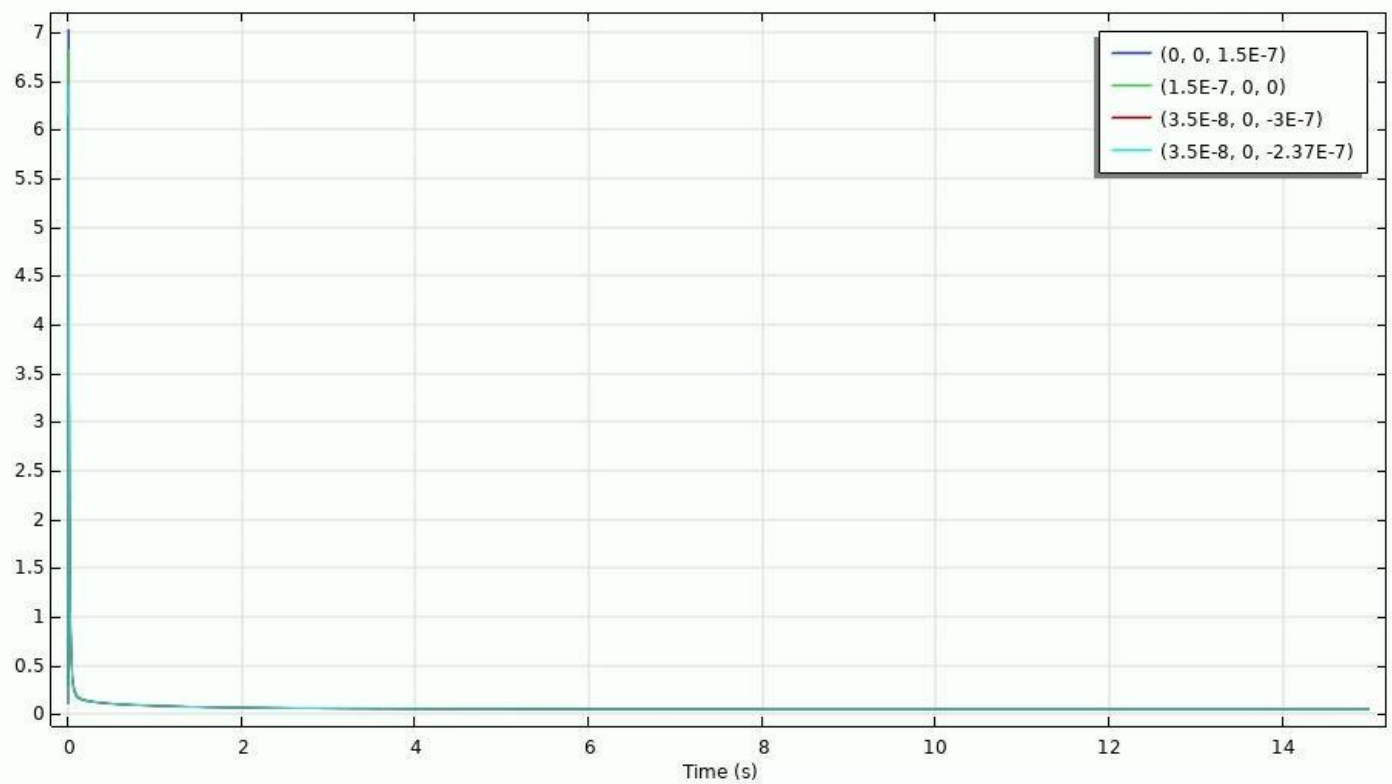


3D plots for Our Modified Sphere in Sphere Model

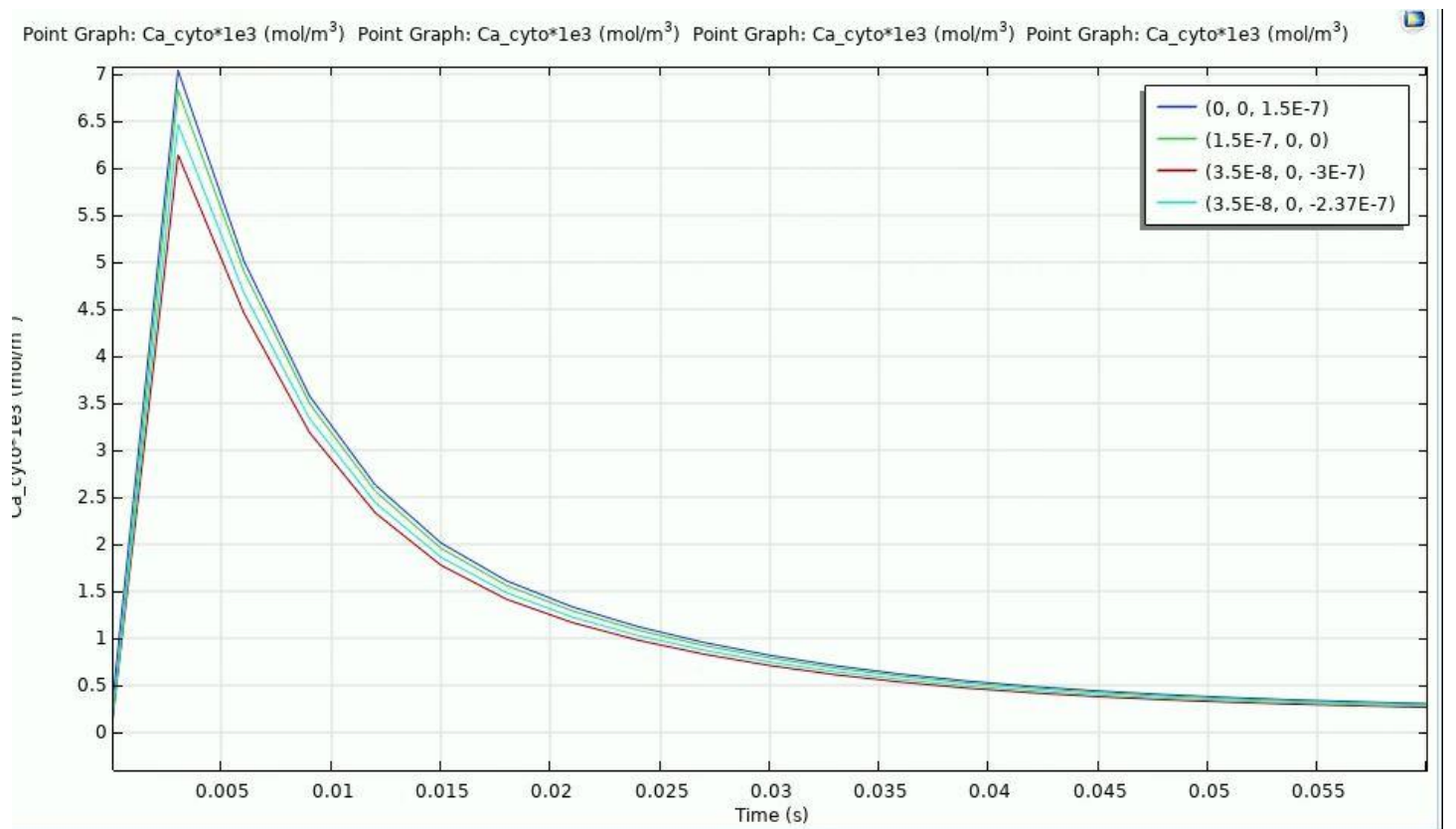


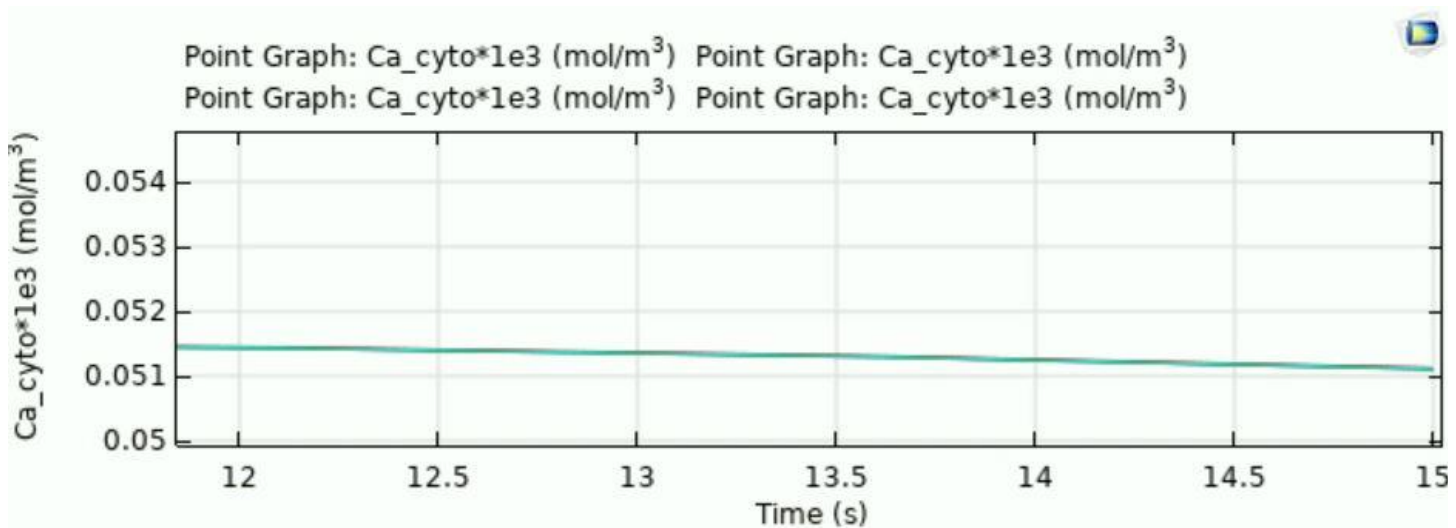


Point Graph: Ca_cyto*1e3 (mol/m³) Point Graph: Ca_cyto*1e3 (mol/m³) Point Graph: Ca_cyto*1e3 (mol/m³) Point Graph: Ca_cyto*1e3 (mol/m³)

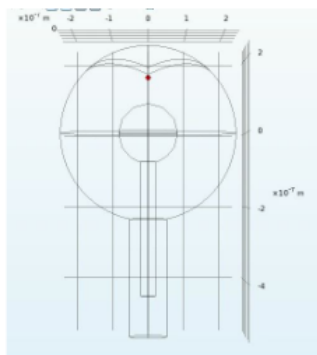


Point Graph: Ca_cyto*1e3 (mol/m³) Point Graph: Ca_cyto*1e3 (mol/m³) Point Graph: Ca_cyto*1e3 (mol/m³) Point Graph: Ca_cyto*1e3 (mol/m³)

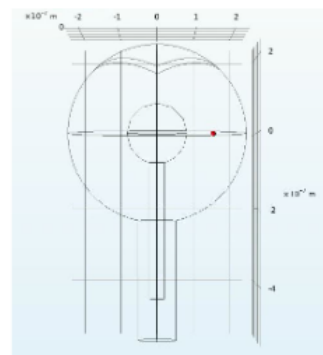




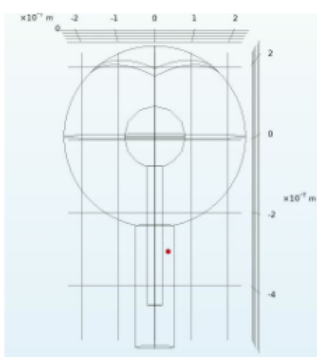
Graphs for the 4 points in the original sphere in sphere



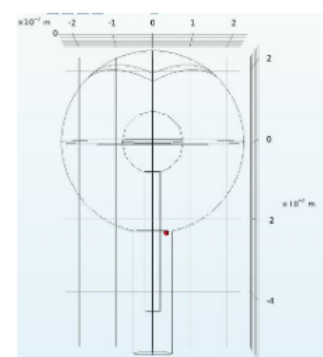
Top Volume



Side Volume

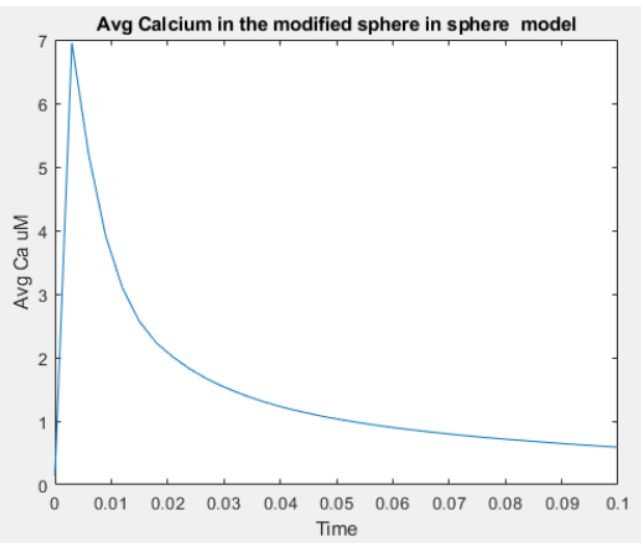
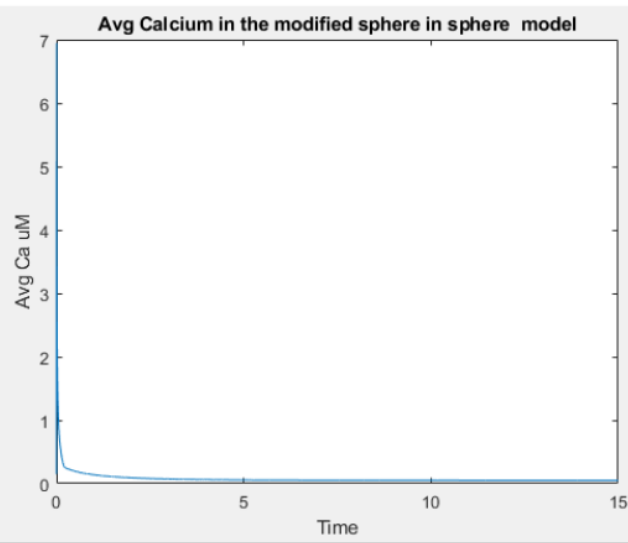
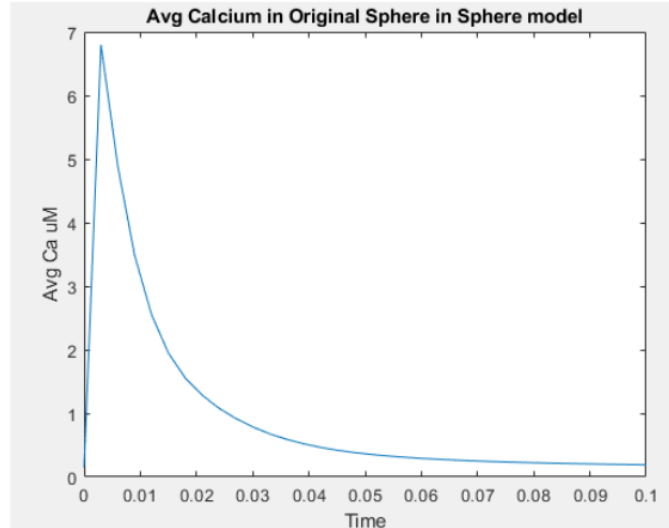
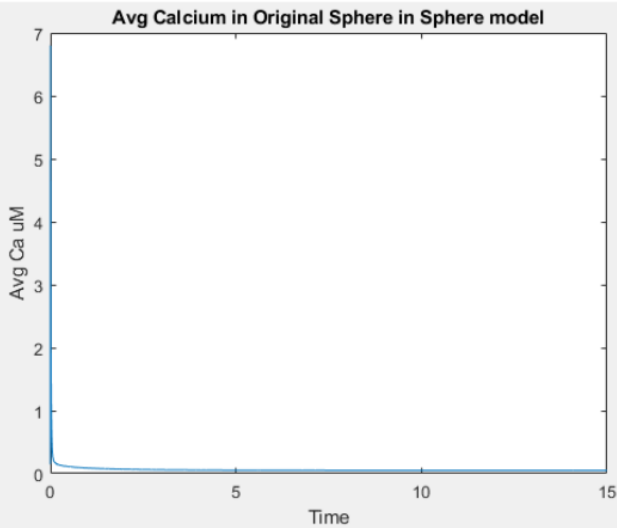


Neck Volume

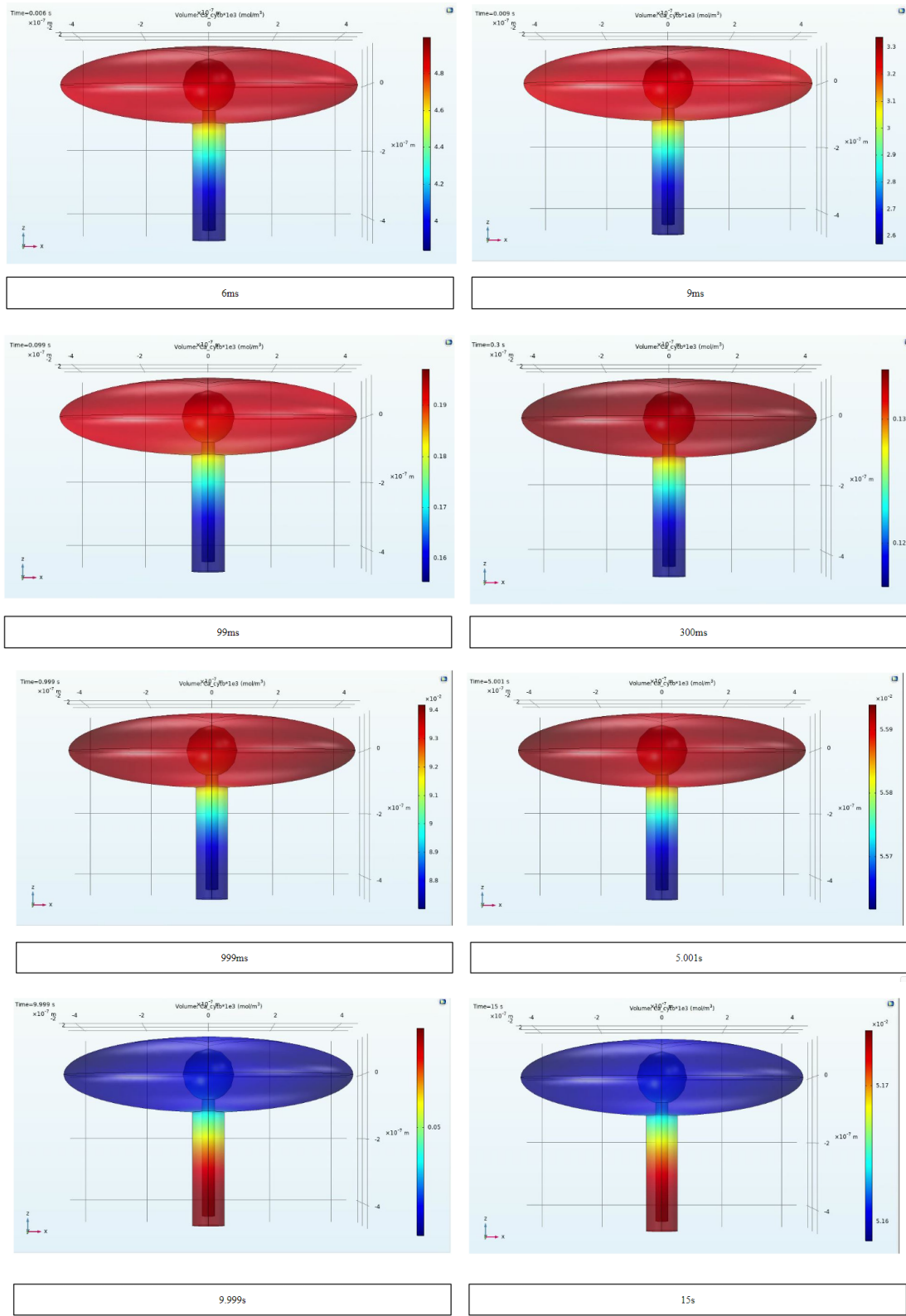


Head-Neck Interface

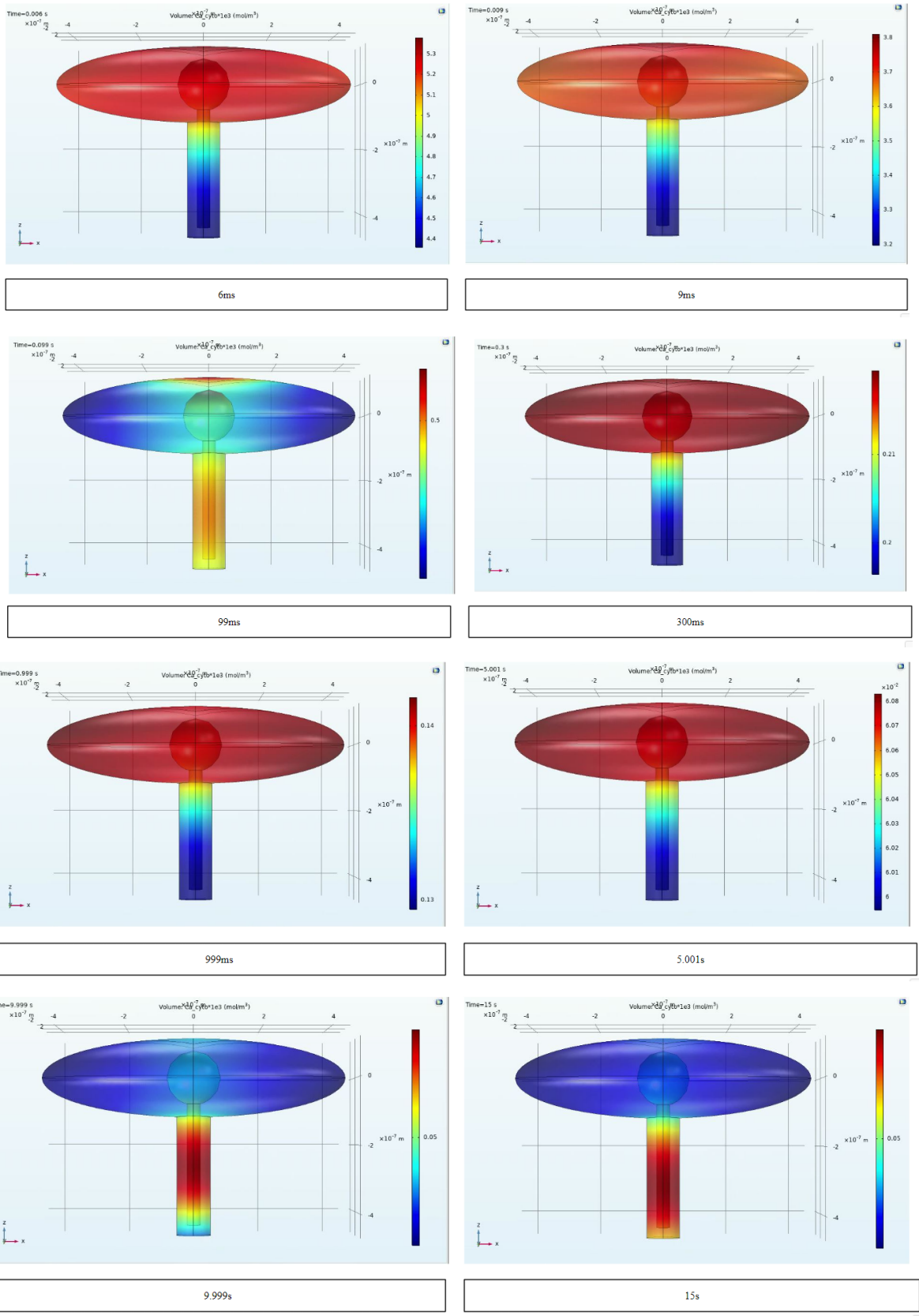
The four points for the graph



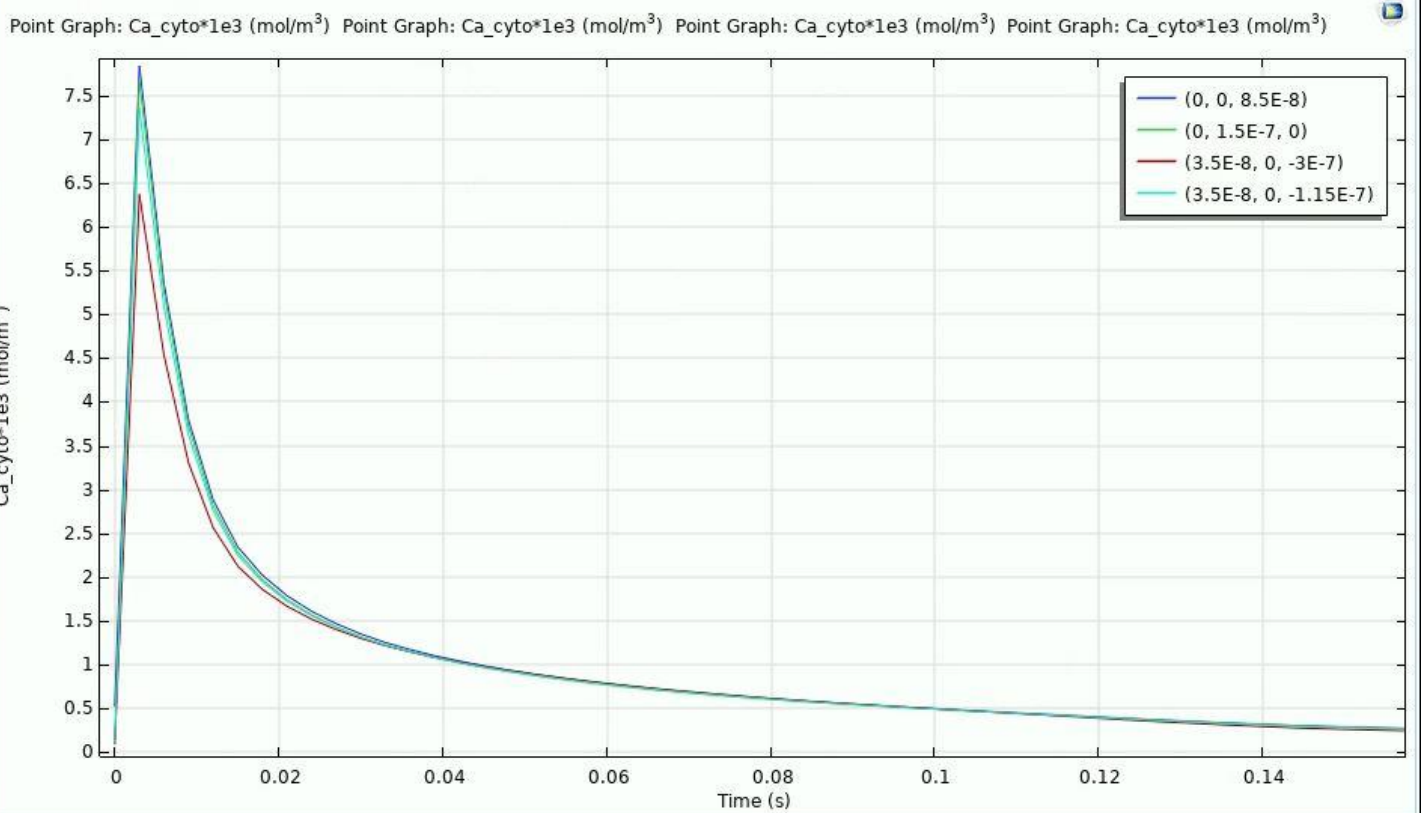
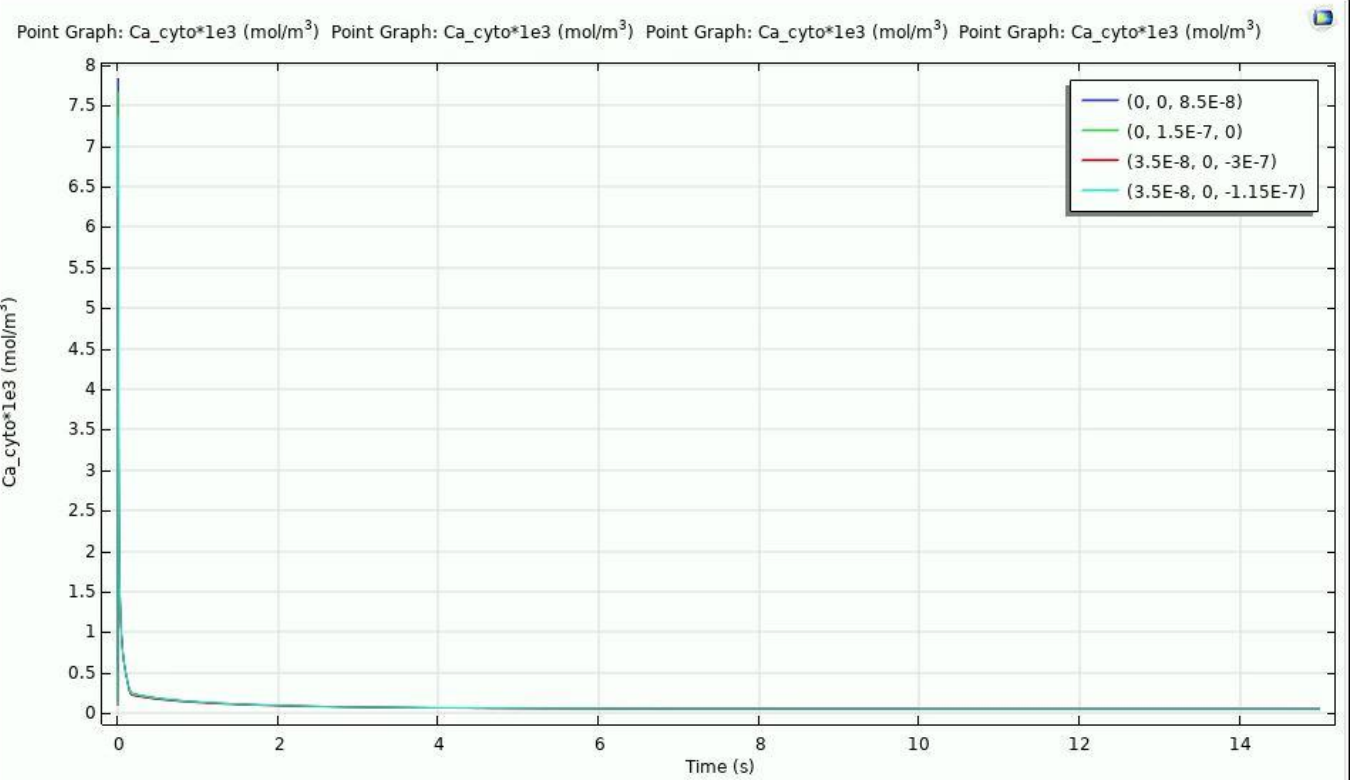
Sphere in Ellipse S5:

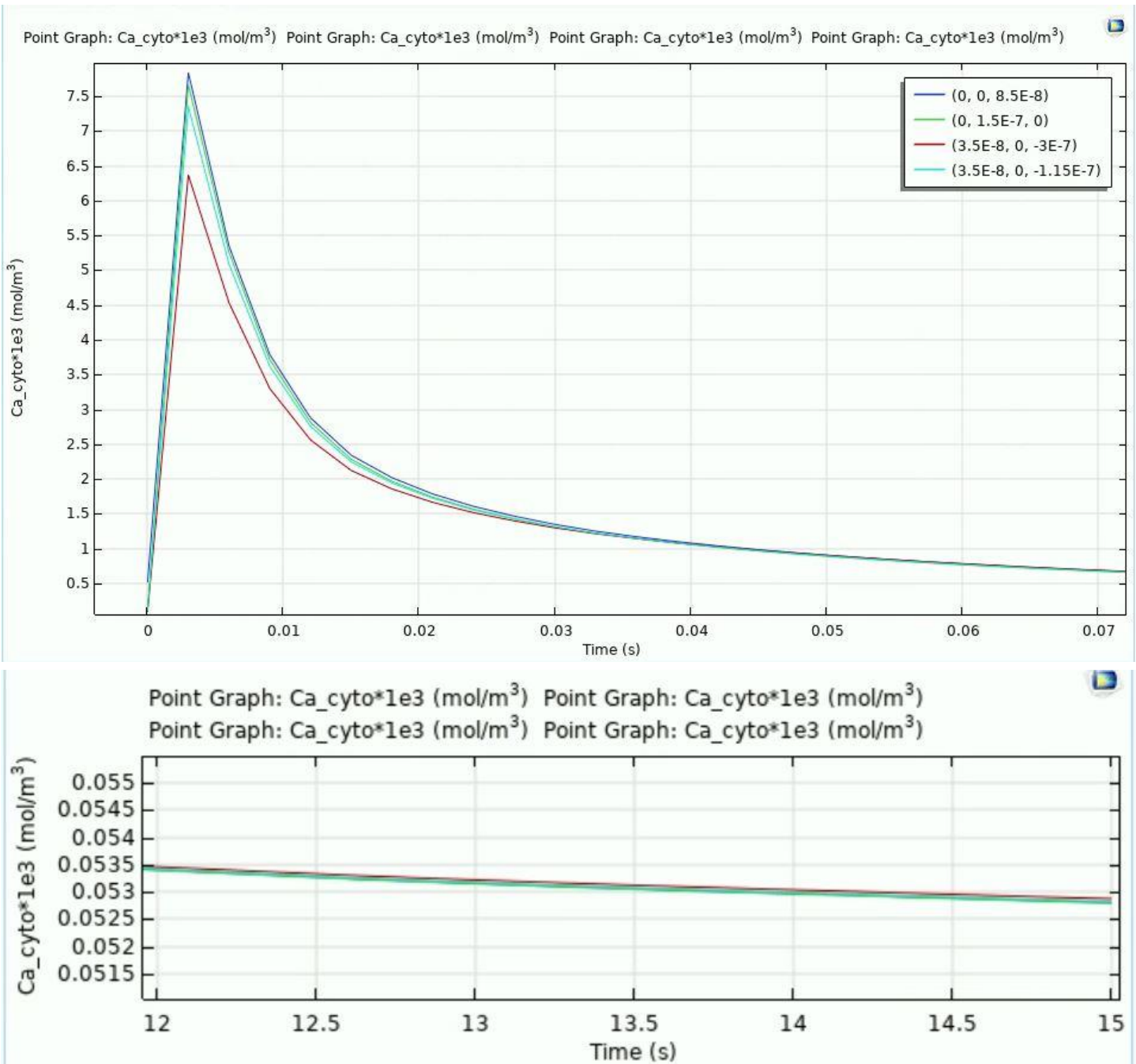


3D plots for the original Sphere in Ellipse Model

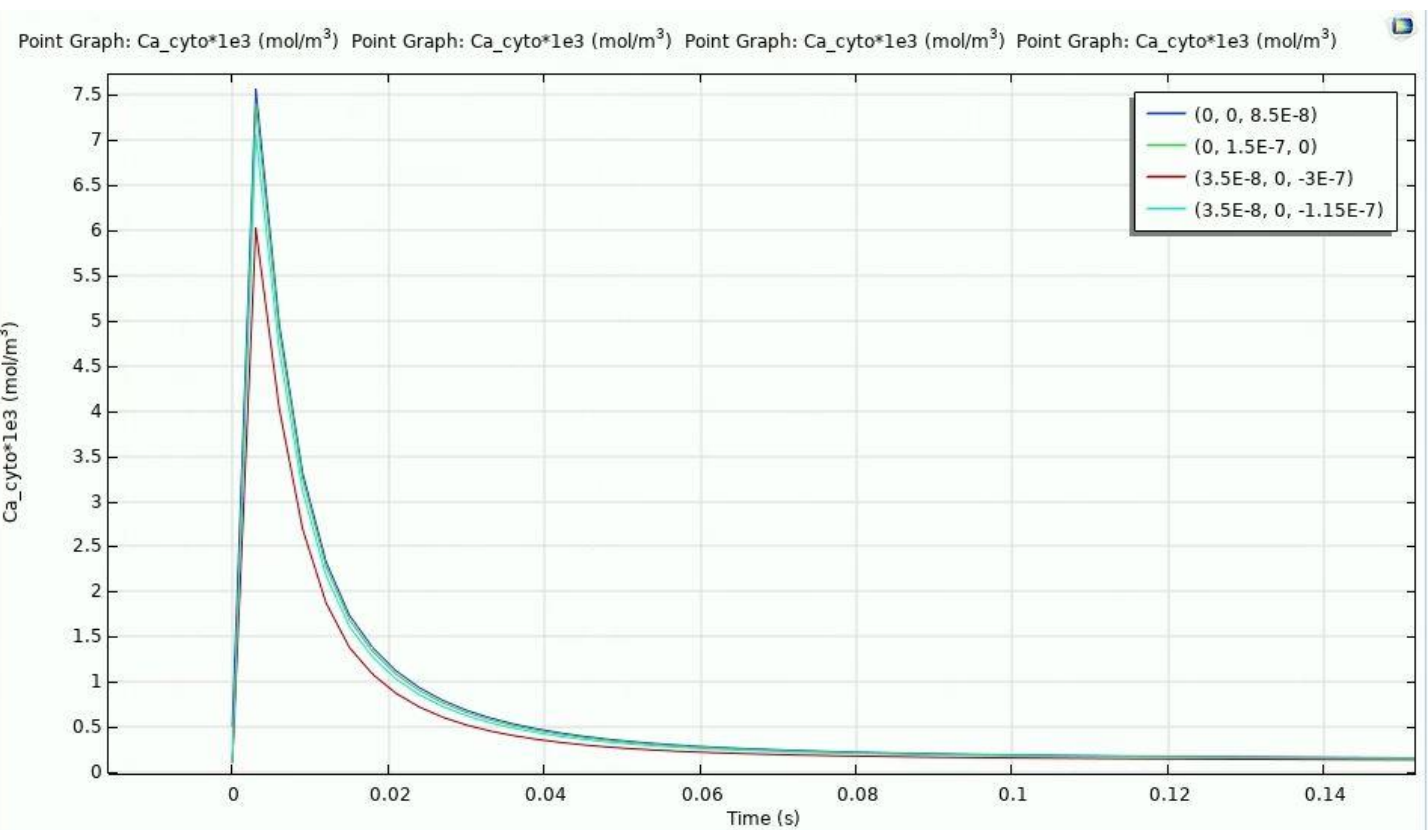
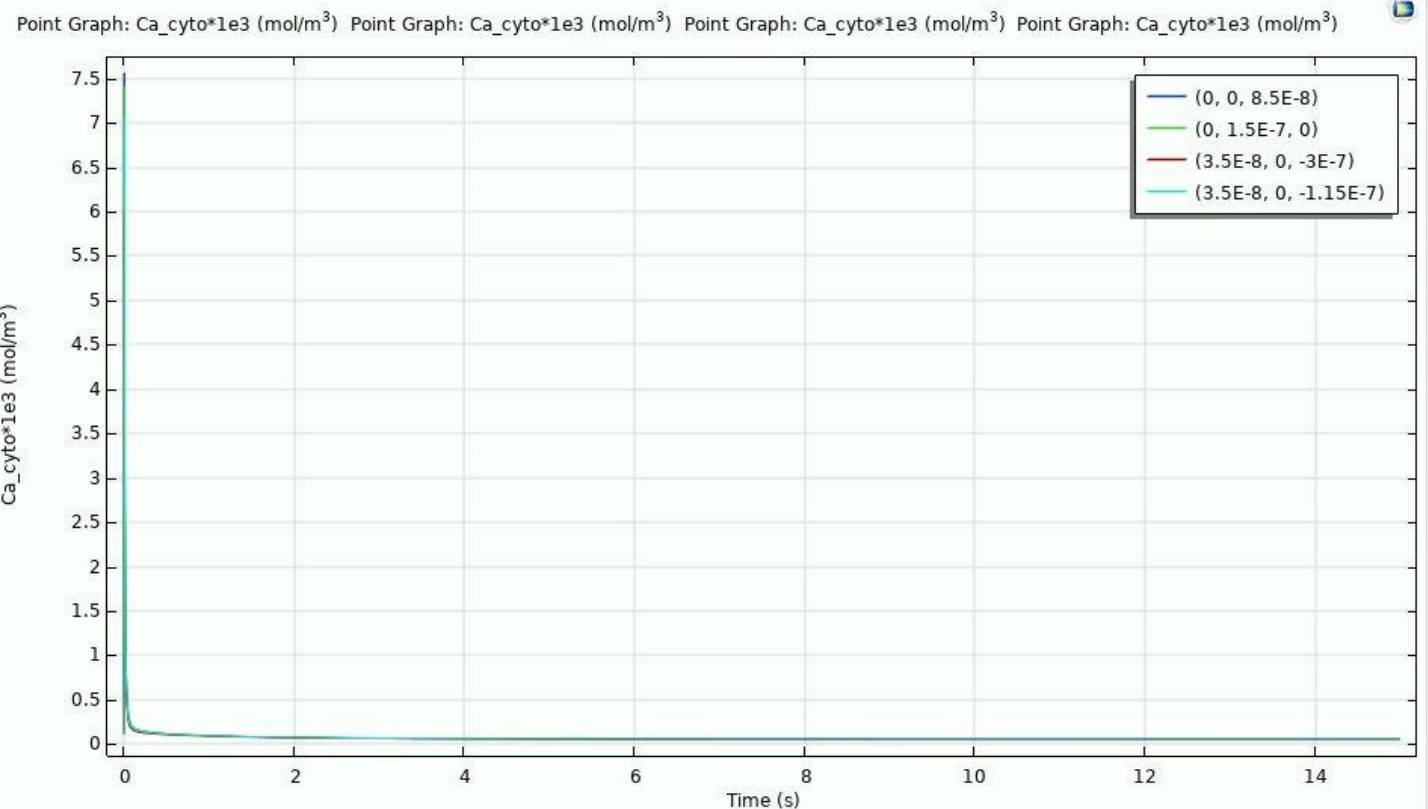


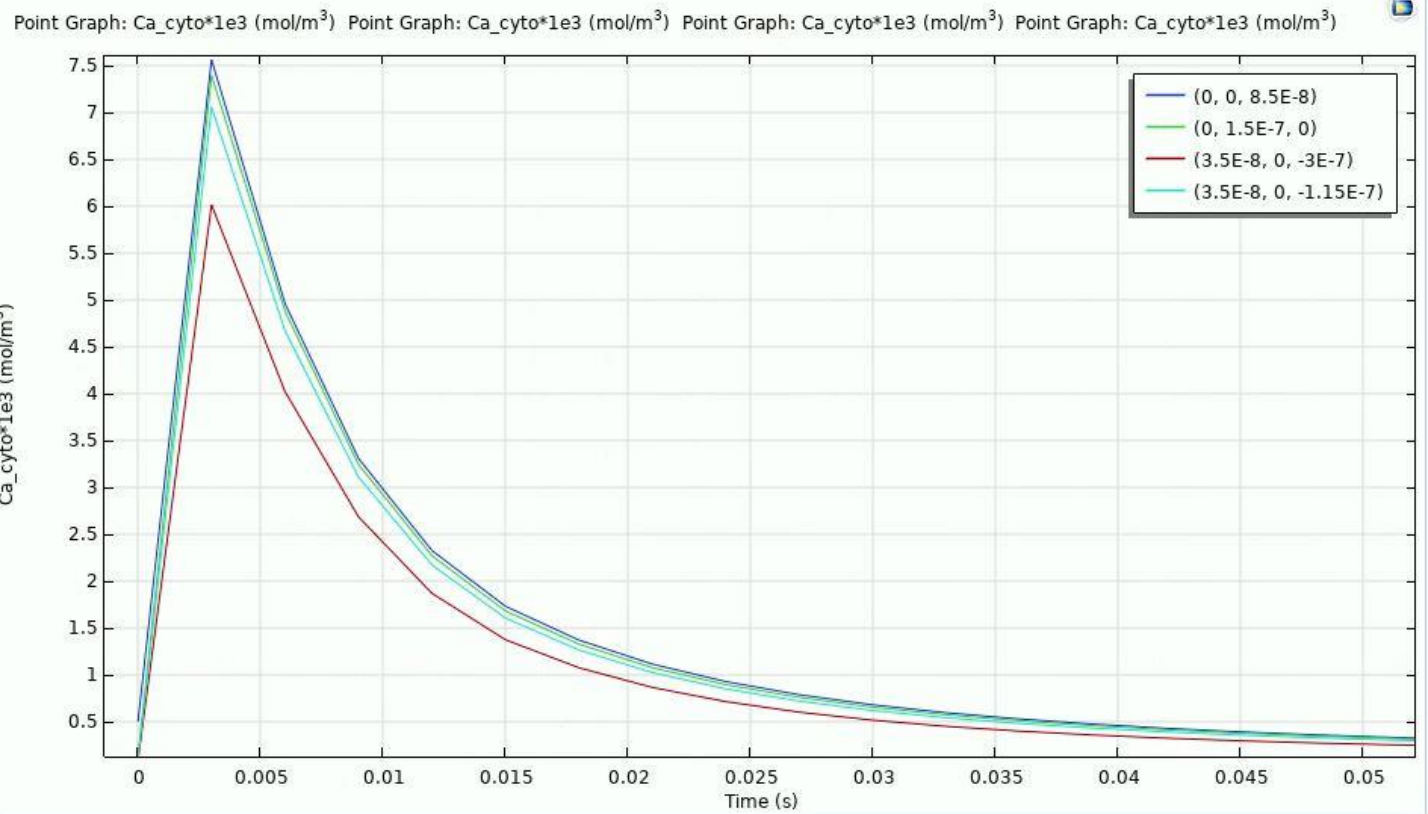
3D plots for the modified Sphere in Ellipse model



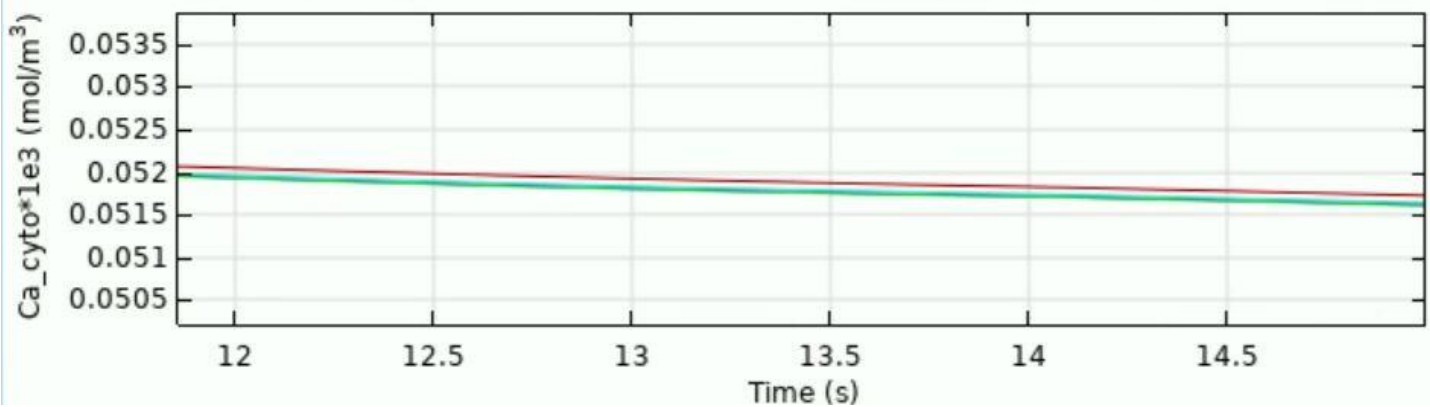


Graphs from the 4 points for modified sphere in ellipse

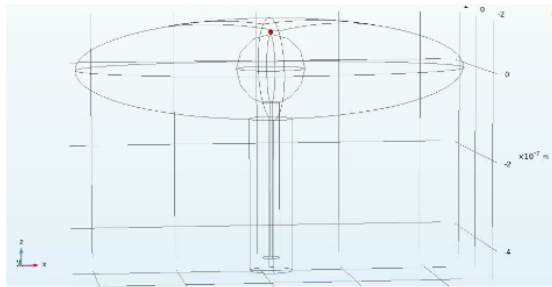




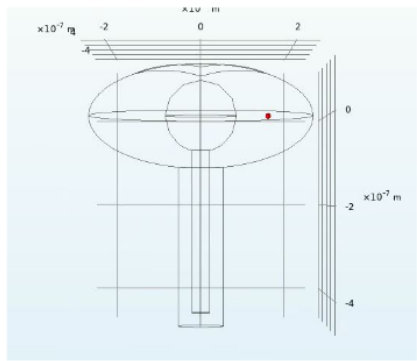
Point Graph: Ca_{cyto}*1e3 (mol/m³) Point Graph: Ca_{cyto}*1e3 (mol/m³)
Point Graph: Ca_{cyto}*1e3 (mol/m³) Point Graph: Ca_{cyto}*1e3 (mol/m³)



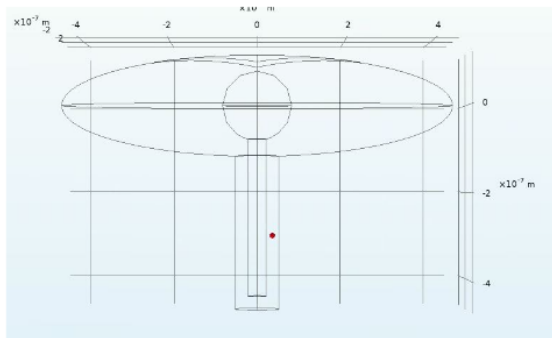
Graphs for the 4 points in the original sphere in ellipse



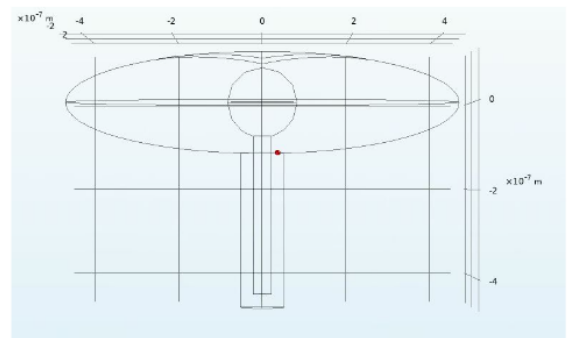
Top Volume



Side Volume

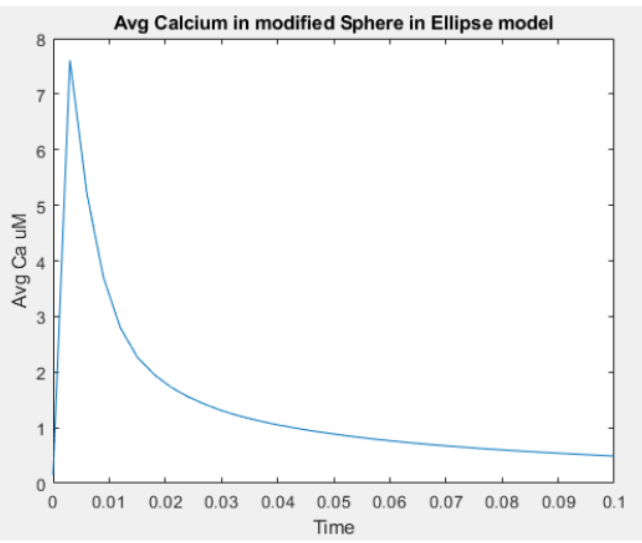
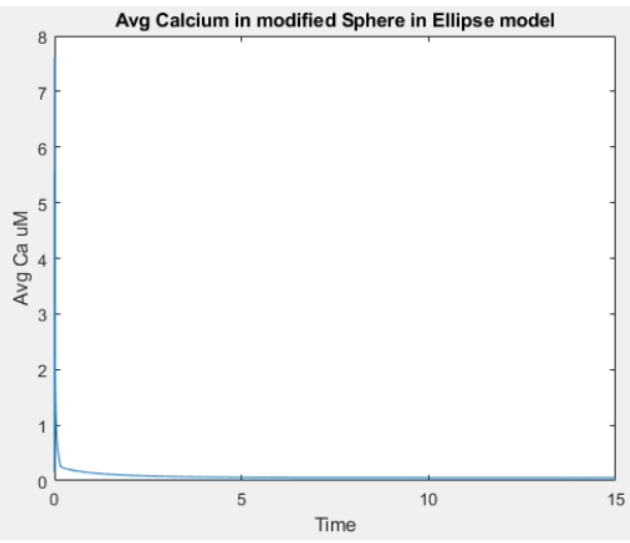
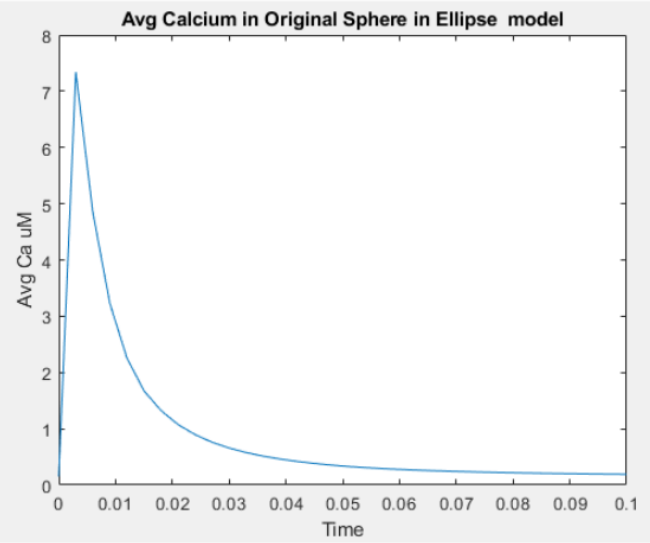
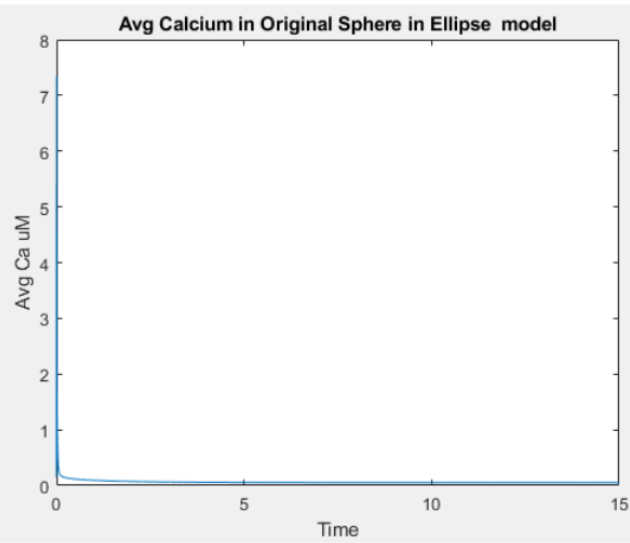


Neck Volume

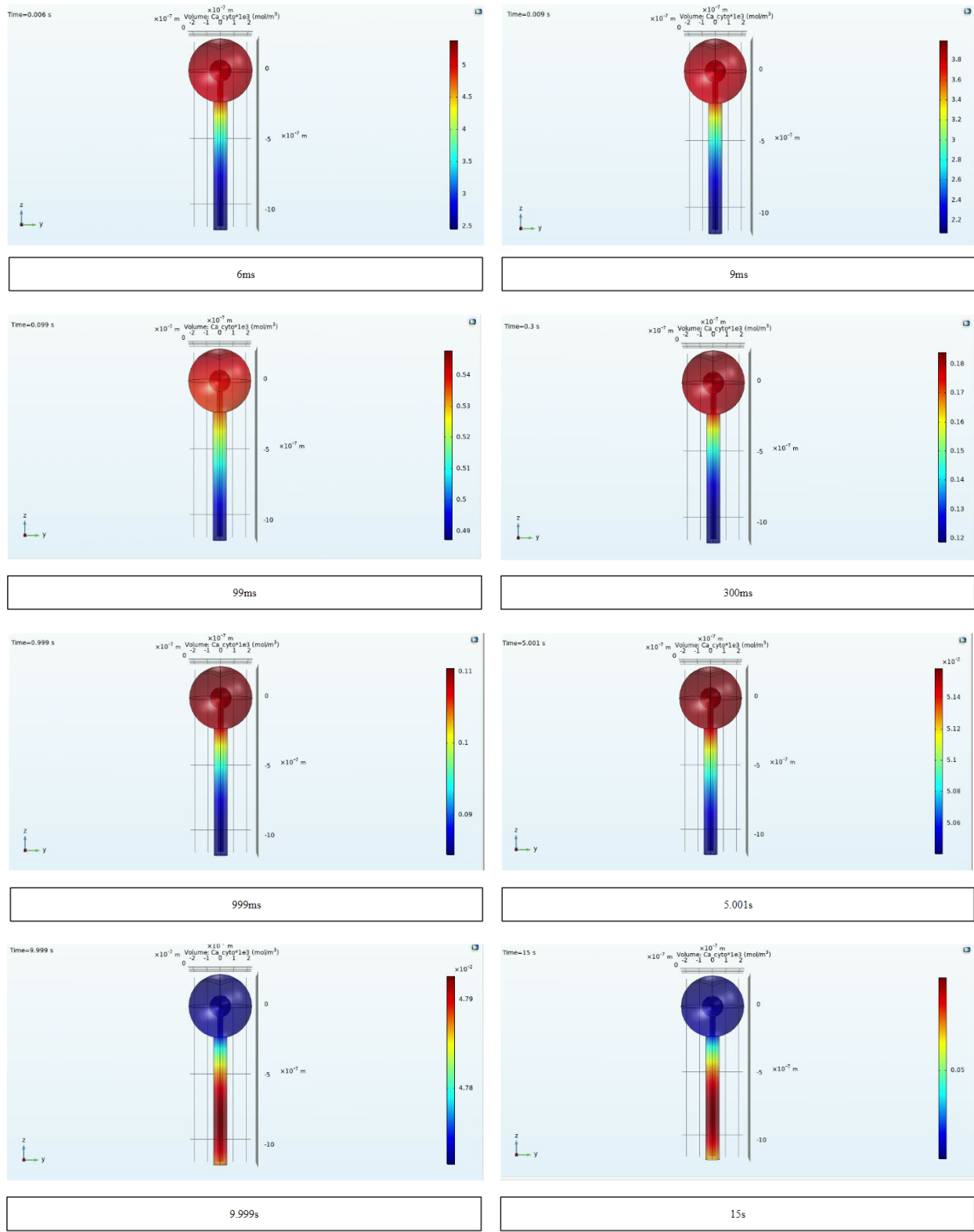


Head-Neck Interface

The points used for the graphs in Figures 5-6 for the Sphere in Ellipse

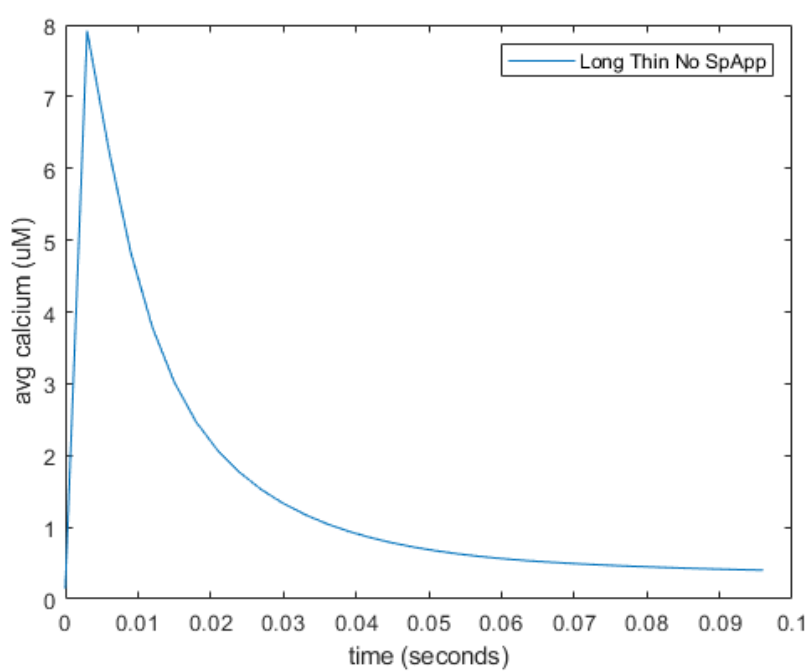
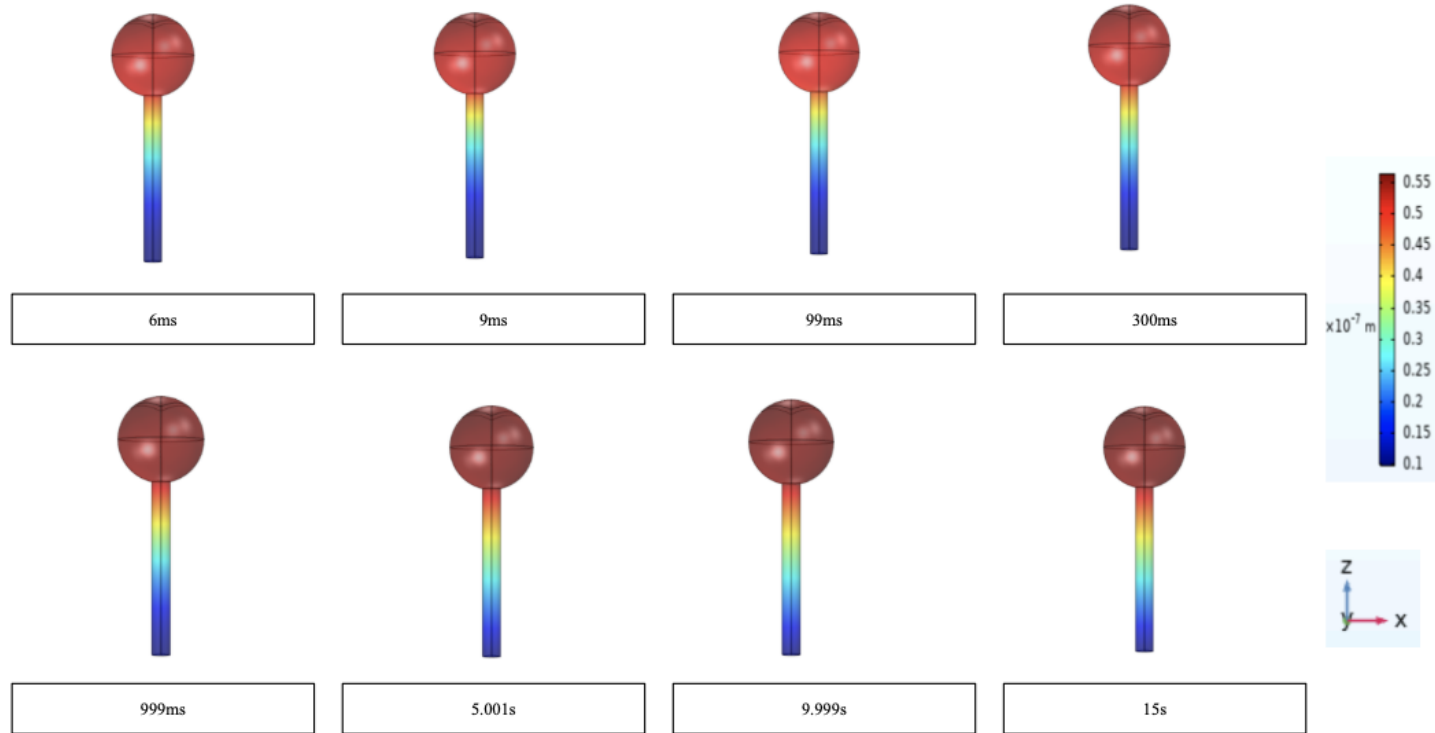


Long Thin Spine Model with SpApp S6



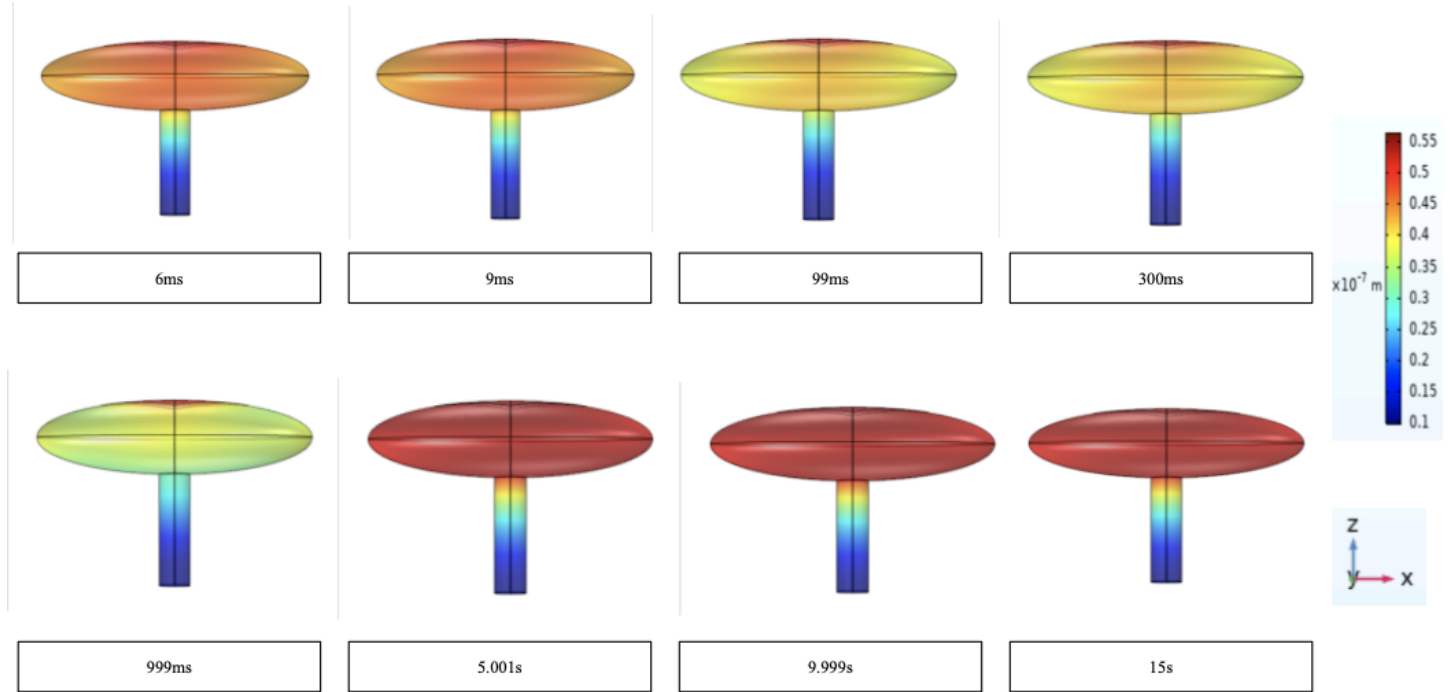
3D plots for the long thin spine with SpApp

Long Thin Spine Model Without SpApp S7

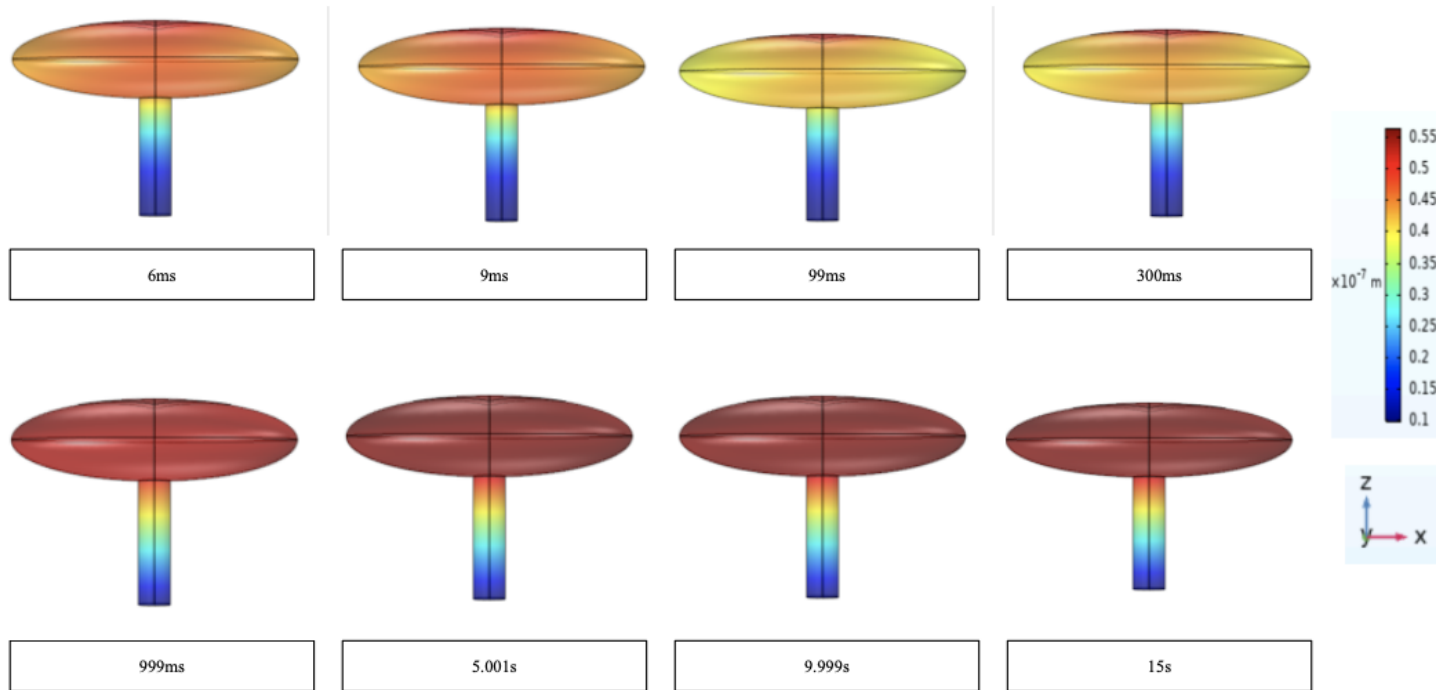


Average calcium in the dendritic spine of the long thin model

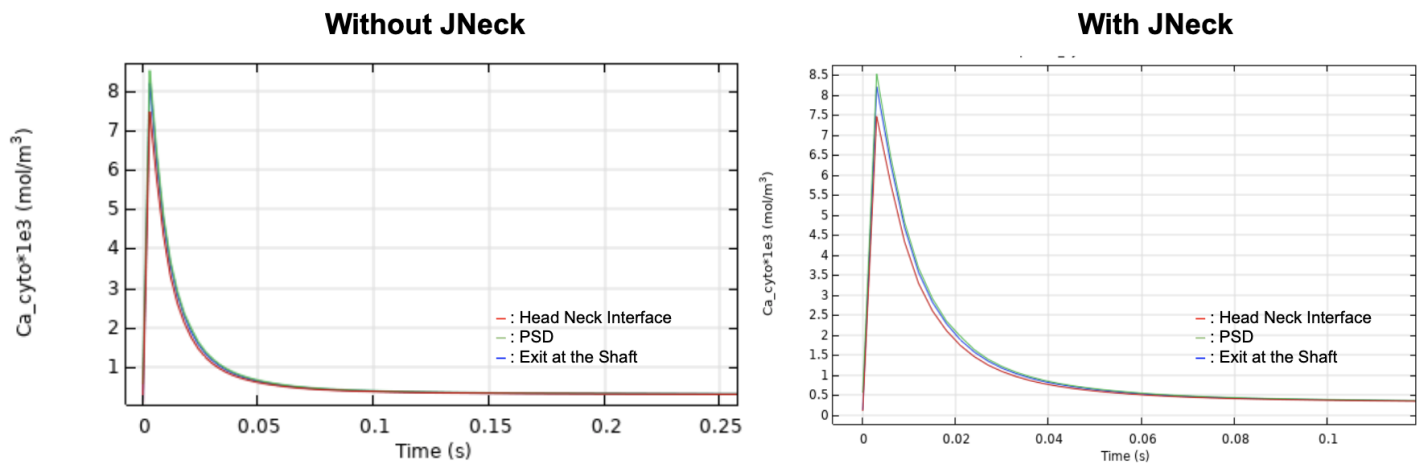
Ellipsoid Without SpApp S8



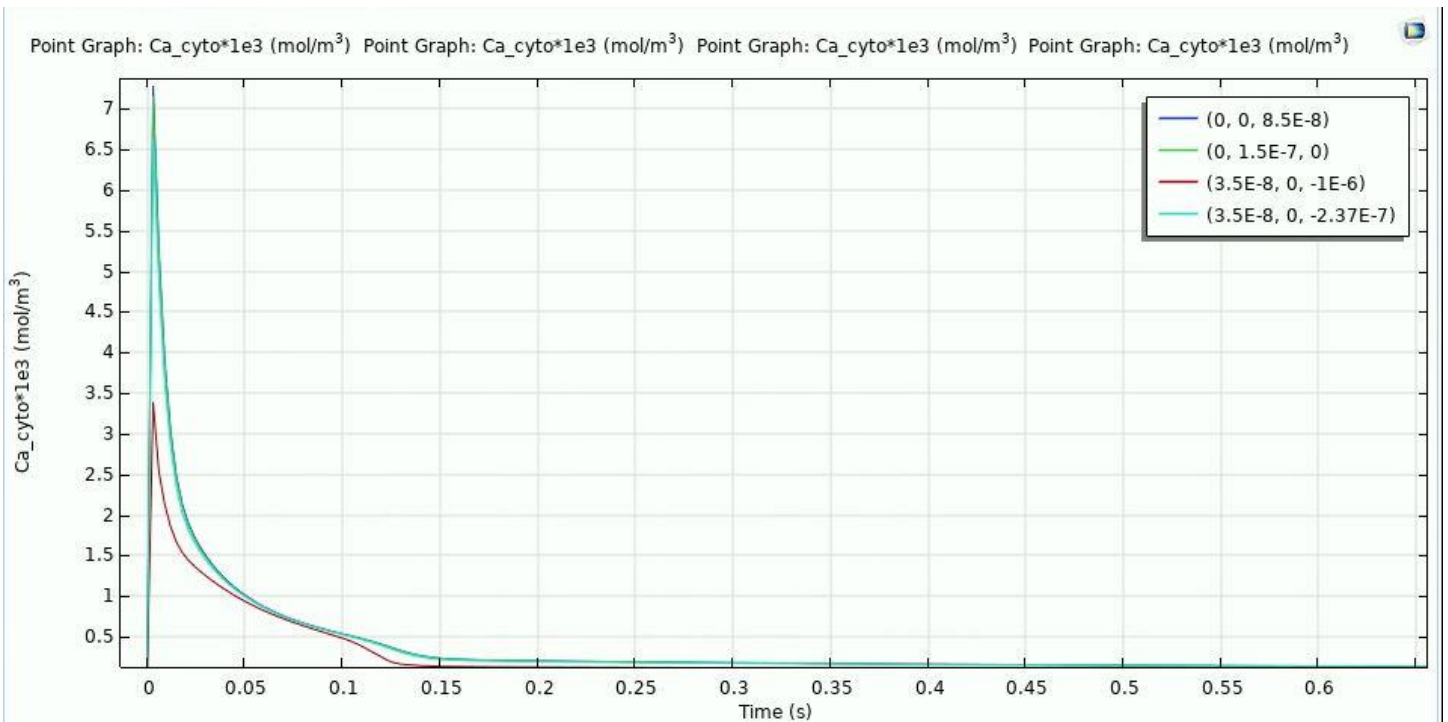
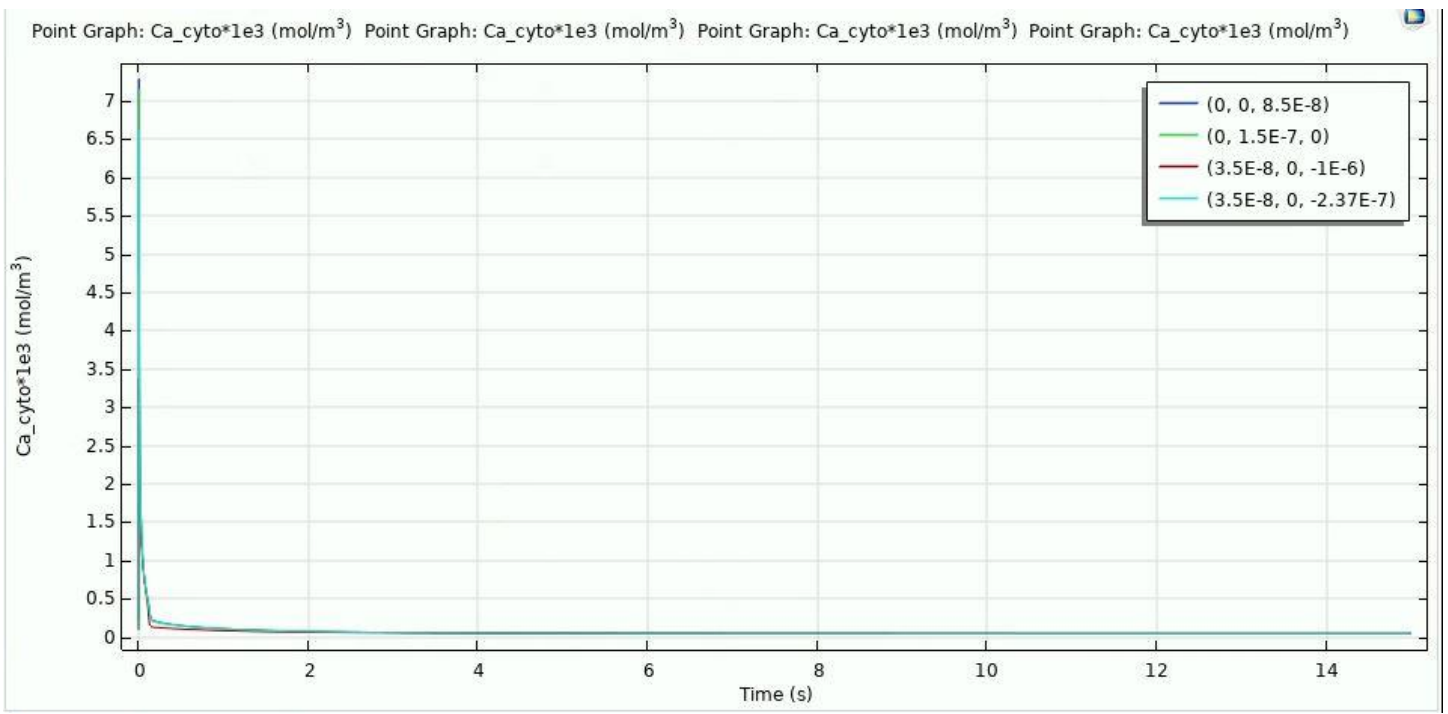
3D plots for the ellipsoid without SpApp and No Neck Efflux



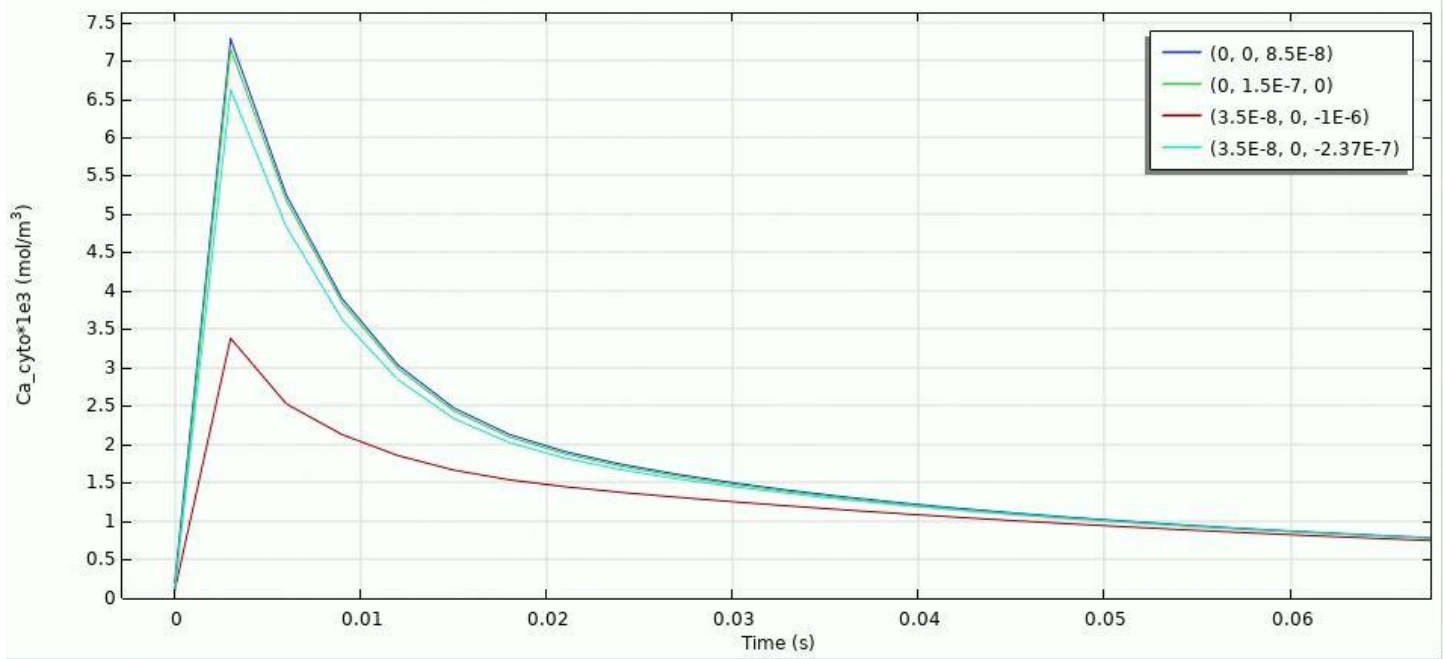
3D plots for the ellipsoid without SpApp and With a Neck Efflux



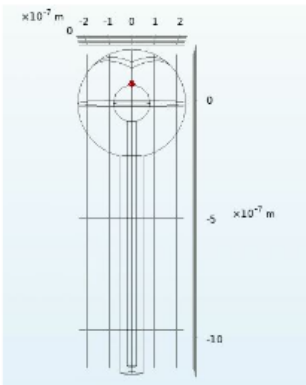
Comparison of the calcium transient at the head and neck interface, the PSD, and the exit at the shaft for the original Ellipsoid model (without the integration of the neck efflux) and the modified Ellipsoid model (with the integration of the the neck efflux).



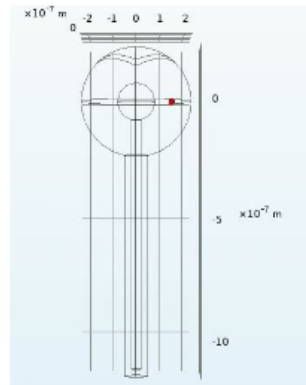
Point Graph: Ca_cyto*1e3 (mol/m³) Point Graph: Ca_cyto*1e3 (mol/m³) Point Graph: Ca_cyto*1e3 (mol/m³) Point Graph: Ca_cyto*1e3 (mol/m³)



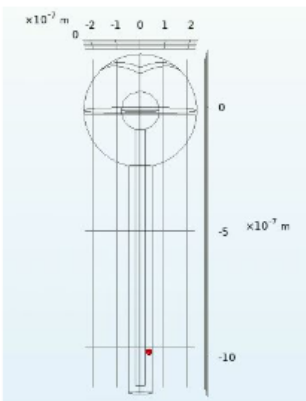
Graphs from the 4 points of the long thin model with SpApp



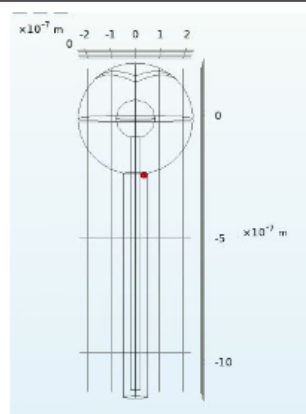
Top Volume



Side Volume

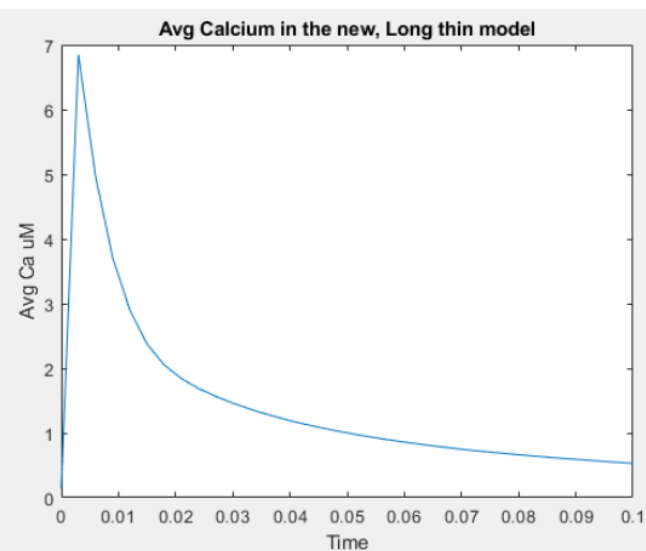
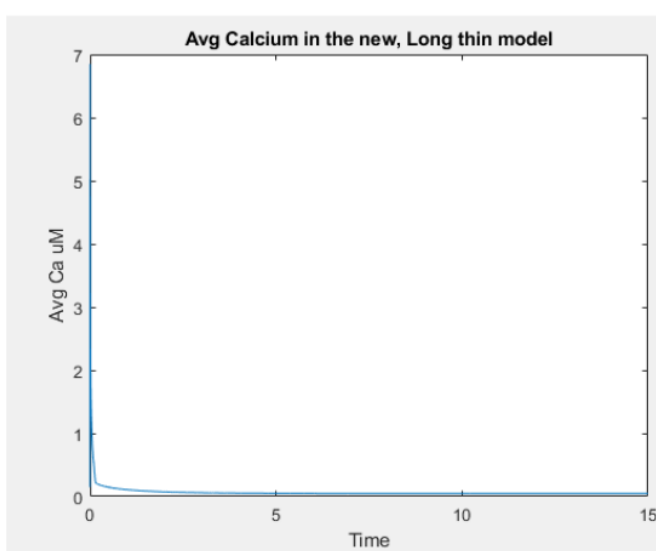


Neck Volume



Head-Neck Interface

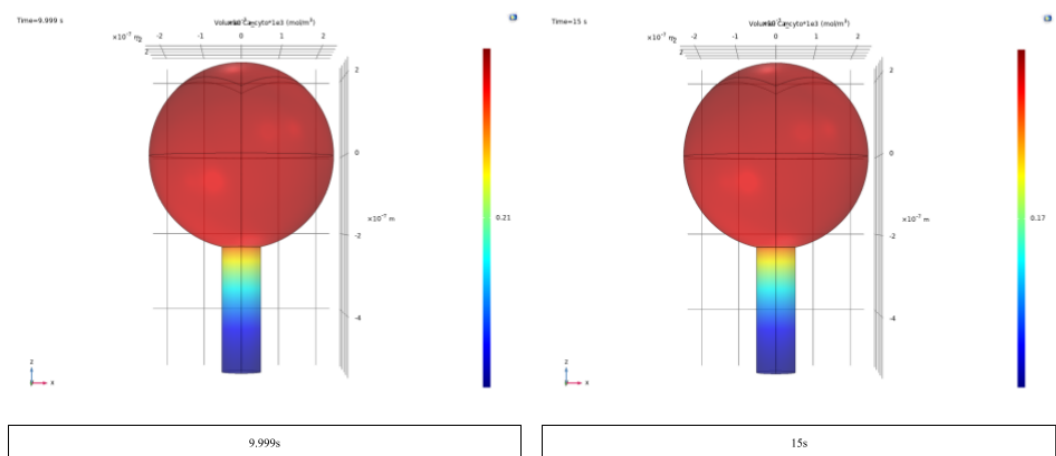
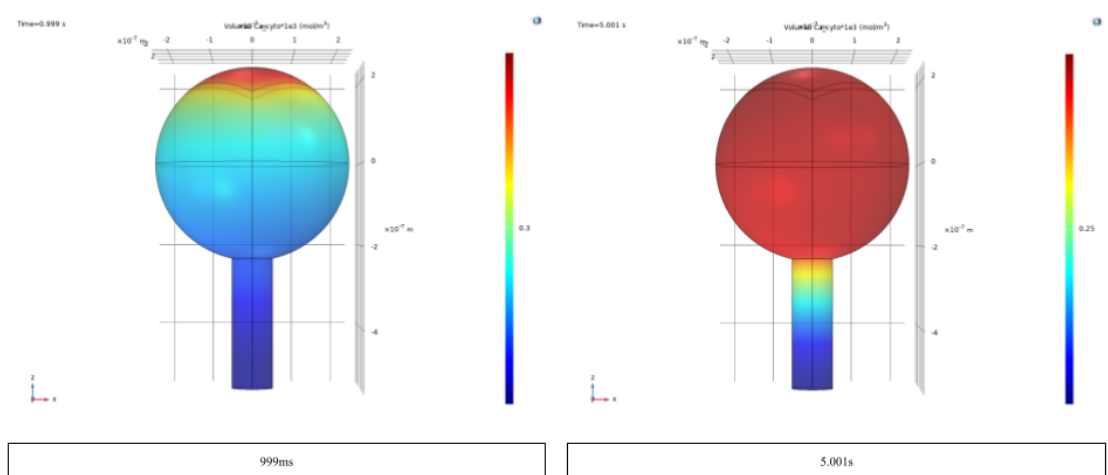
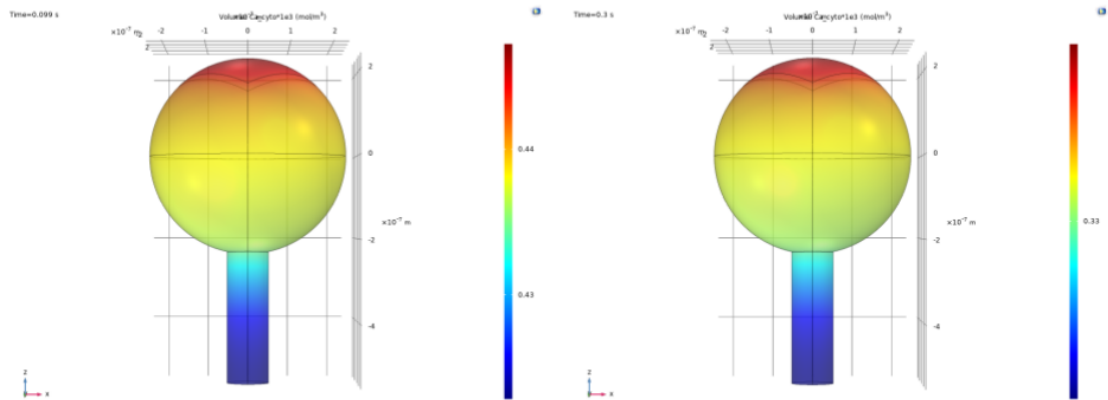
Where the 4 points for the graphs are



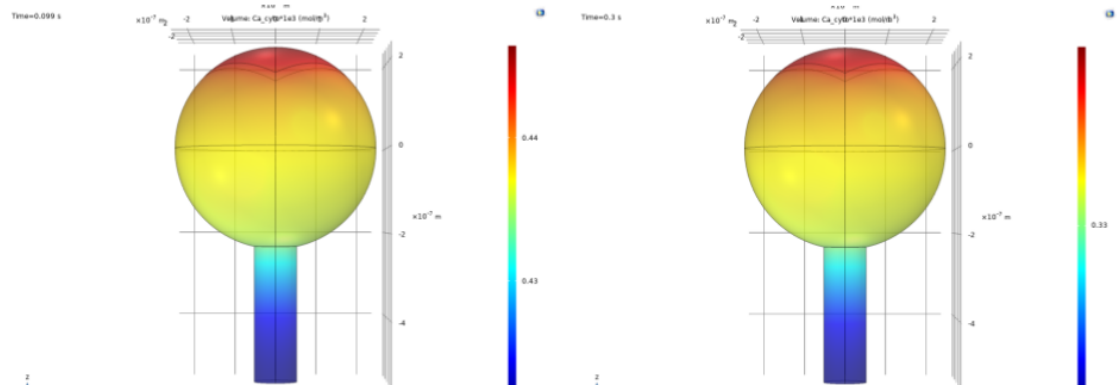
S9: Sphere without Spine Apparatus

Modified model with inclusion Neck Flux into dendrite proper

Original without Neck Flux

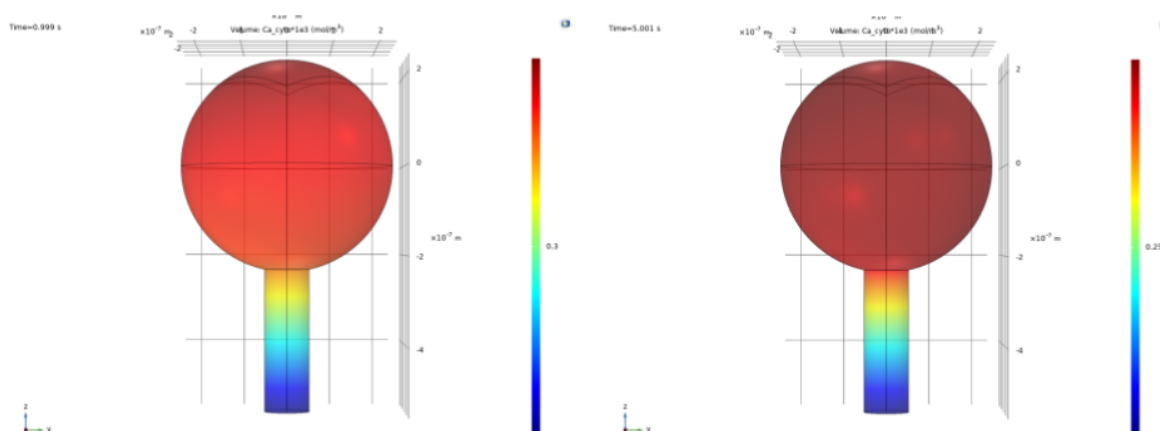


Modified with Neck Flux



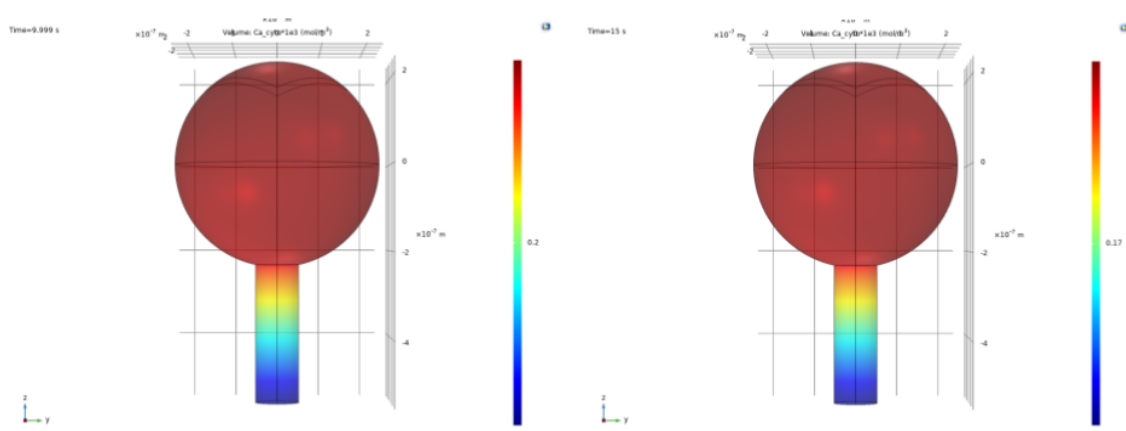
99ms

300ms



999ms

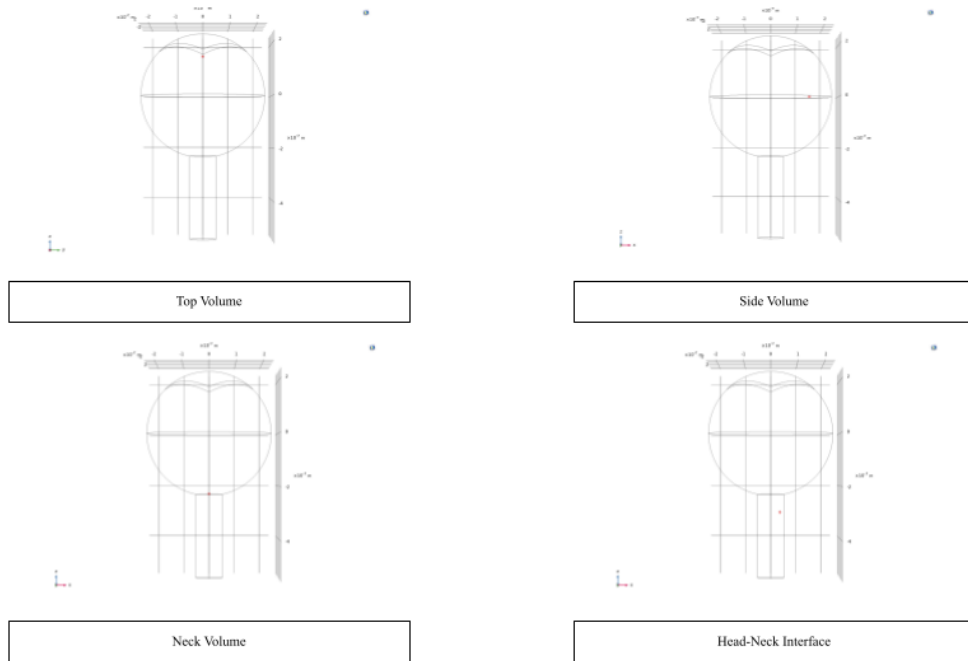
5.001s



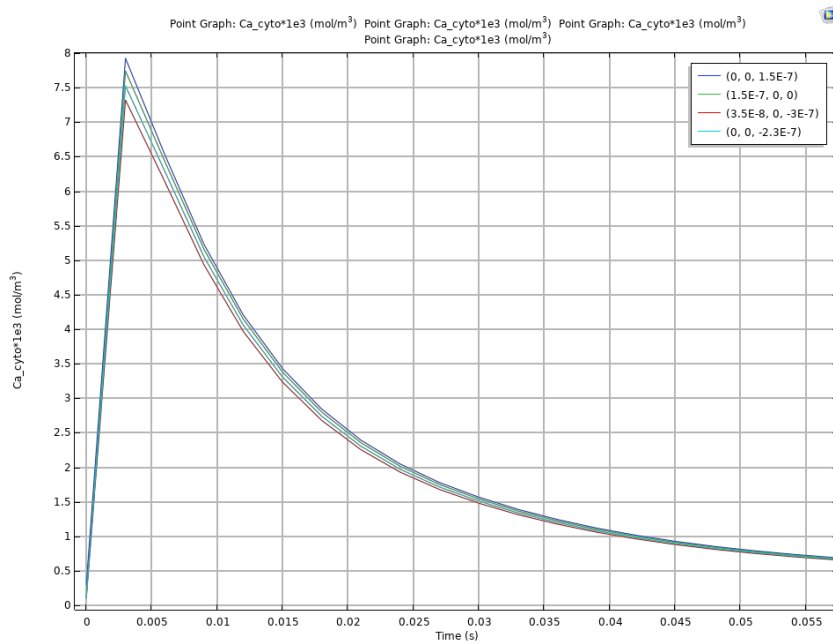
9.999\$

15s

The figures above indicate that there is little change to the distribution and concentration of calcium in cytosol with the inclusion of neck calcium flux. From the assumptions made in the methods section we see that the neck flux is negligible at short time-scales. It is apparent that longer time-scales do have an effect on calcium transience through the neck and into the dendrite. At around 15 seconds we begin to see a further distribution of calcium down the neck in the modified model than in the original, indicative of calcium flowing into and out of the spine neck and into the dendrite.



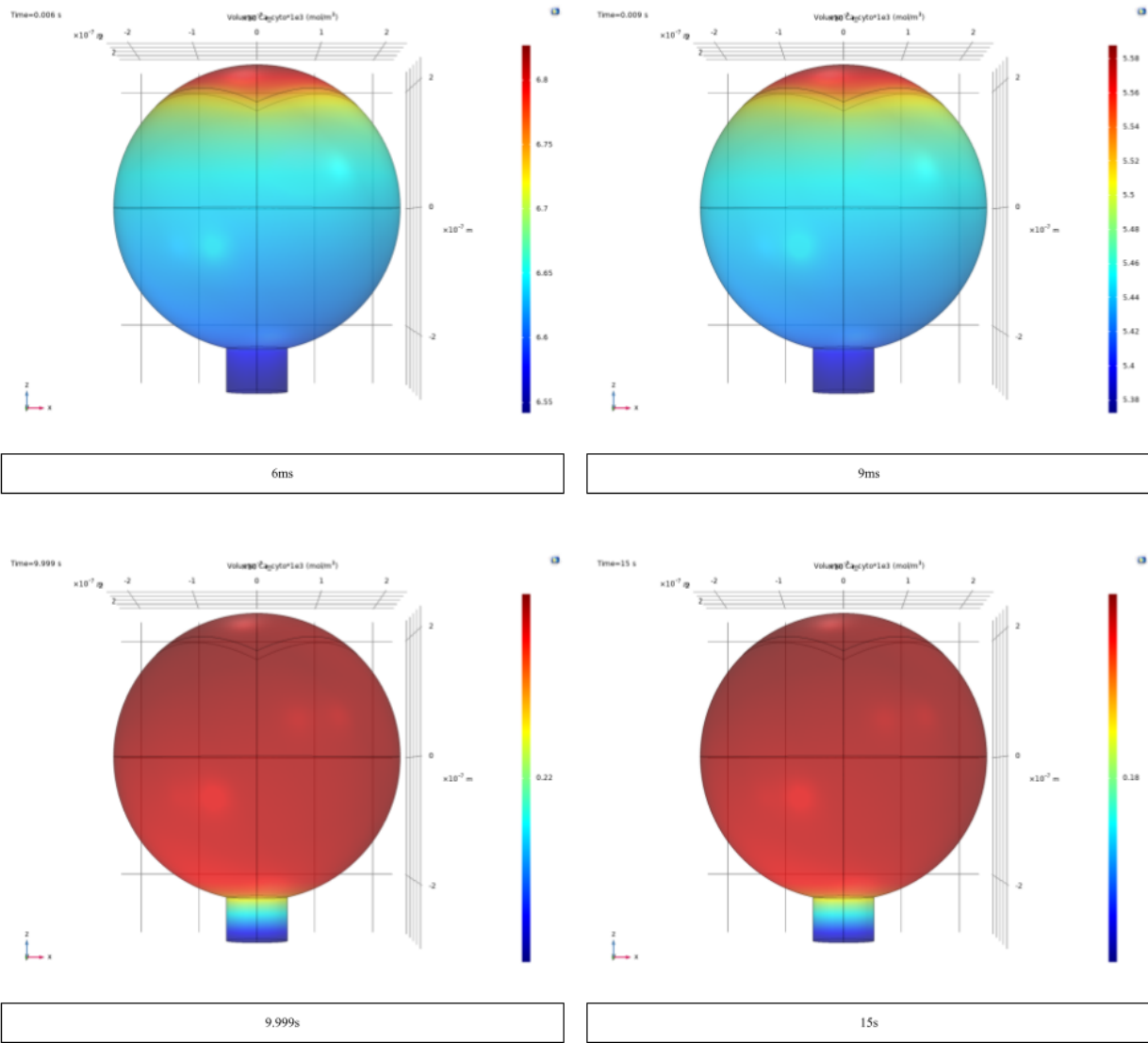
Location of point value within the 3D model



Graphs of concentration at set locations in the model (Top, Side, Neck, Neck-Head Interface (Top to bottom)).
The left is the original model and the right is the modified model with Neck flux.

There appears to be little effect from adding a set neck flux alone. In combination with other parameters and time-scales there could be a larger impact on calcium transience within the dendritic spine. This concludes that, for short time-scales, the assumptions made in the original model, namely, fixing flux through the base of the neck to zero, was adequate.

Stubby



The graphs above for the stubby model geometries shine light on the aspects of dendritic spine neck transience. It appears that the head fills rather quickly with calcium and then slowly trickles through the neck, at a much lower rate and time-scale.

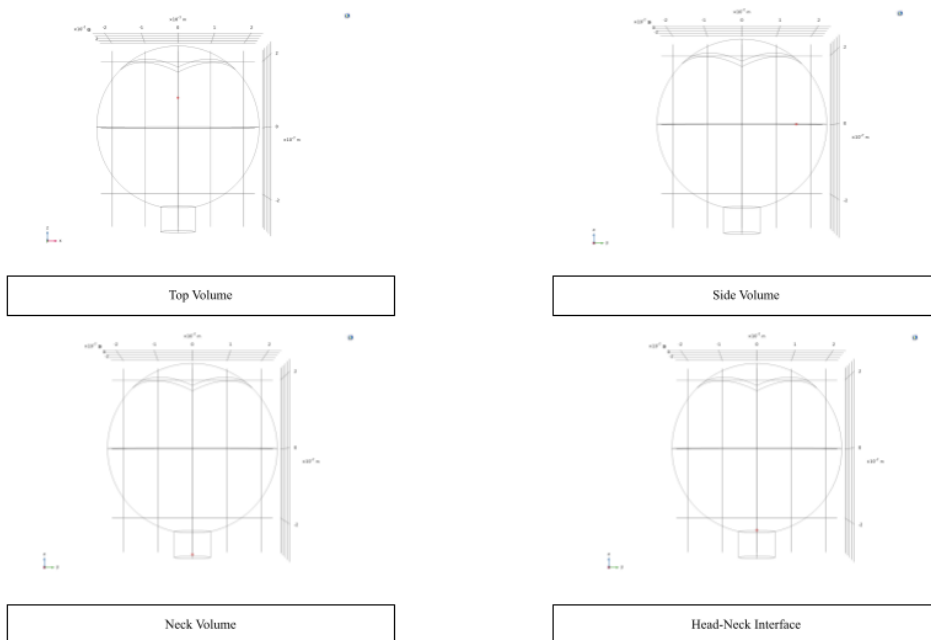
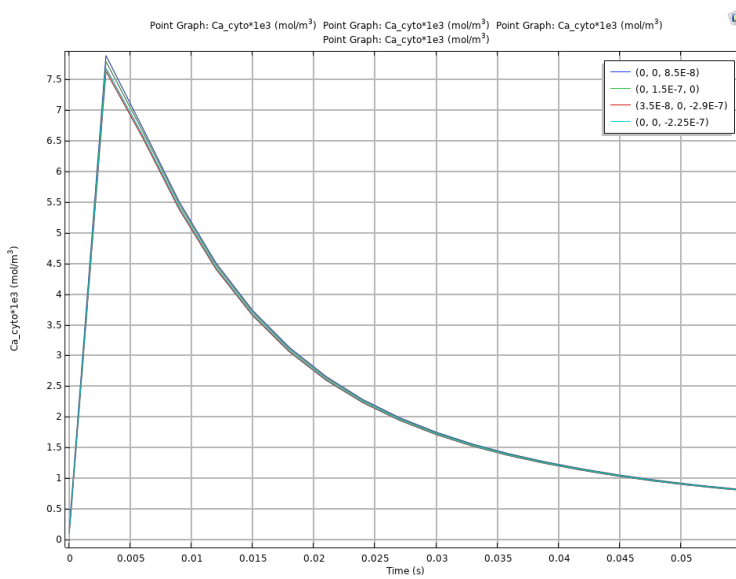
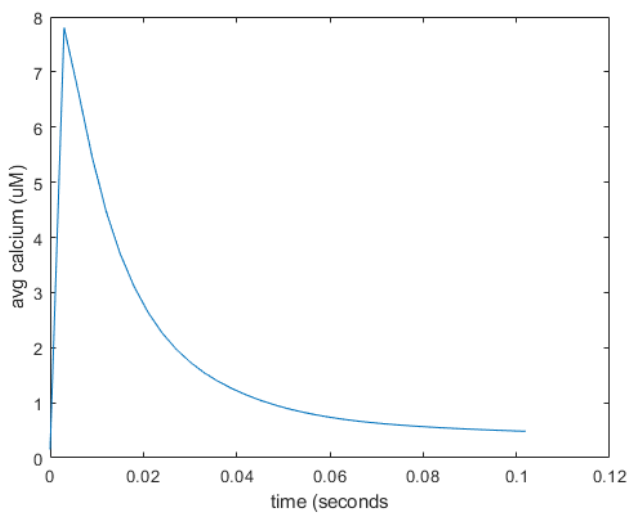


Diagram of the location of point graphs for the stubby model

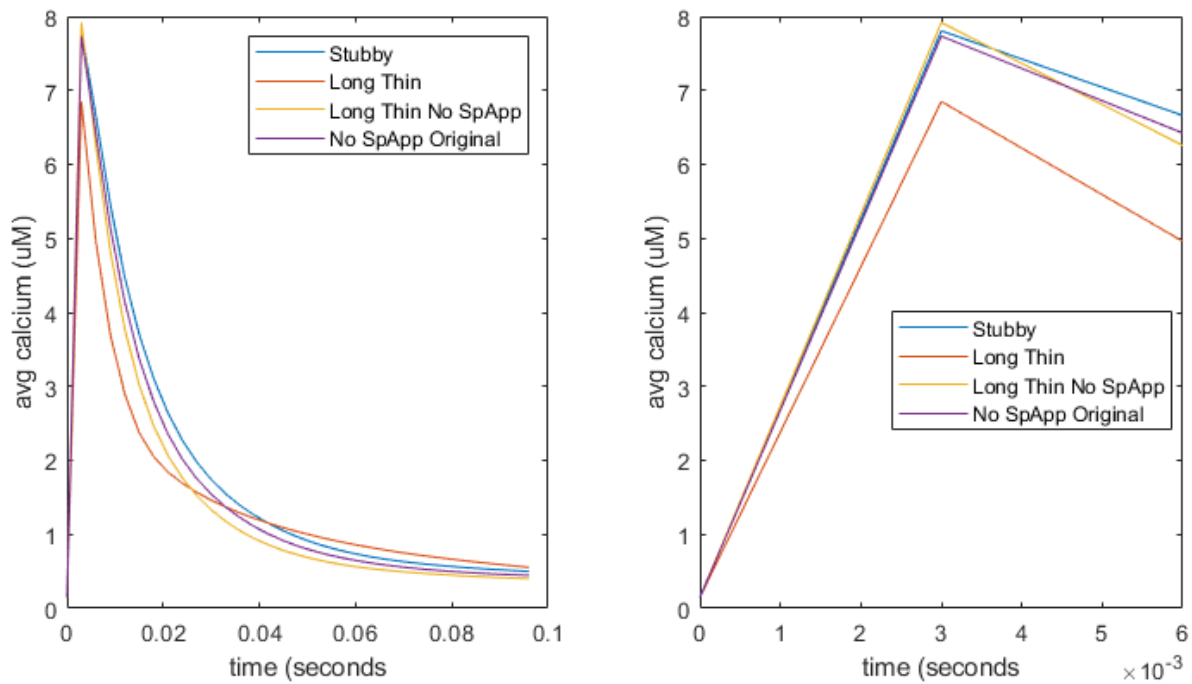


Calcium transience at different locations in the stubby dendritic spine model (Top, Side, Neck, Head-Neck Interface [top to bottom])



Average calcium in the stubby dendritic spine model

S11: Modified Geometries



Modified geometries and the average calcium concentrations over time. Blue is the stubby, red is long thin with a spine apparatus, yellow is the long thin without a spine apparatus, and purple is the original spine without a spine apparatus.

Model	Peaks (μM)	Time Constant (ms)
Original Spherical without SpApp	7.729	14.6
Stubby	7.804	16.7
Long Thin with SpApp	6.847	9.5
Long Thin without SpApp	7.917	12.1